LAPPEENRANTA
UNIVERSITY OF TECHNOLOGY

Katri Sirola

CHELATING ADSORBENTS IN PURIFICATION OF HYDROMETALLURGICAL SOLUTIONS

Thesis for the degree of Doctor of Science (Technology) to be presented with due permission for public examination and criticism in the Auditorium of the Student Union House at Lappeenranta University of Technology, Lappeenranta, Finland on the 11th of December, 2009 at noon.

Acta Universitatis
Lappeenrantaensis
360

Supervisor
Professor Erkki Paatero
Department of Chemical Technology
Lappeenranta University of Technology
Finland

Reviewers
Professor Jukka Lehto
Department of Chemistry
University of Helsinki
Finland

Professor Arup K Sengupta
Department of Chemical Engineering
Lehigh University, Bethlehem, Pennsylvania 18015
USA

Opponent
Professor Nalan Kabay
Chemical Engineering Department
Ege University, Bornova, Izmir
Turkey

Custos
Professor Erkki Paatero
Department of Chemical Technology
Lappeenranta University of Technology
Finland

ISBN 978-952-214-842-1
ISBN 978-952-214-843-8 (PDF)
ISSN 1456-4491

Lappeenrannan teknillinen yliopisto
Digipaino 2009

ABSTRACT

Katri Sirola

Chelating Adsorbents in Purification of Hydrometallurgical Solutions

Lappeenranta 2009
63 pages

Acta Universitatis Lappeenrantaensis 360
Diss. Lappeenranta University of Technology

ISBN 978-952-214-843-8 (PDF), ISBN 978-952-214-842-1, ISSN 1456-4491

In this thesis, equilibrium and dynamic sorption properties of weakly basic chelating adsorbents were studied to explain removal of copper, nickel from a concentrated zinc sulfate solution in a hydrometallurgical process. Silica-supported chelating composites containing either branched poly(ethyleneimine) (BPEI) or 2-(aminomethyl)pyridine (AMP) as a functional group were used. The adsorbents are commercially available from Purity Systems Inc, USA as WP-1® and CuWRAM®, respectively. The fundamental interactions between the adsorbents, sulfuric acid and metal sulfates were studied in detail and the results were used to find the best conditions for removal of copper and nickel from an authentic $ZnSO_4$ process solution. In particular, the effect of acid concentration and temperature on the separation efficiency was considered. Both experimental and modeling aspects were covered in all cases.

Metal sorption is considerably affected by the chemical properties of the studied adsorbents and by the separation conditions. In the case of WP-1, acid affinity is so high that column separation of copper, nickel and zinc has to be done using the adsorbent in base-form. On the other hand, the basicity of CuWRAM is significantly lower and protonated adsorbent can be used. Increasing temperature decreases the basicity and the metals affinity of both adsorbents, but the uptake capacities remain practically unchanged. Moreover, increasing temperature substantially enhances intra-particle mass transport and decreases viscosities thus allowing significantly higher feed flow rates in the fixed-bed separation.

The copper selectivity of both adsorbents is very high even in the presence of a 250-fold excess of zinc. However, because of the basicity of WP-1, metal precipitation is a serious problem and therefore only CuWRAM is suitable for the practical industrial application. The optimum temperature for copper removal appears to be around 60 ^{o}C and an alternative solution purification method is proposed. The Ni/Zn selectivity of both WP-1 and CuWRAM is insufficient for removal of the very small amounts of nickel present in the concentrated $ZnSO_4$ solution.

Keywords: Chelating adsorbent, Hydrometallurgy, Solution purification, Zinc Sulfate, Dynamic column separation.

UDC 661.183.1: 669.053.4

ACKNOWLEDGEMENTS

This thesis is a part of two research projects; "the Future Zinc Process (FUZIP) project" of former Outokumpu company with financial support from the National Technology Agency (TEKES) and "Fast, Selective and Ecological Ion Exchange Materials for Hydrometallurgy (FSE-IX) project which is part of Finnish Academy "Sustainable Production and Products (KETJU)"-programme (2006-2010).

First, I want to express my greatest gratitude to my supervisor Prof. Erkki Paatero, who led me to the interesting world of ion exchange and hydrometallurgy, gave me an opportunity to make this challenging study and, first of all, believed in me and my ability to survive such an enormous task. Furthermore, I thank him for many interesting and exhilarating discussions on various topics of this study.

Mr. Markku Laatikainen, I want to give you my highest and warmest compliments for being teacher on the way to the degree of doctor of science and to competence as a scientific researcher. Without your momentous ideas, criticism and assistance, the period of working with this study would not have been as inspiring and rewarding as it has been, when I have had an opportunity to work with you.

I thank the reviewers, Prof. Arup. K. Sengupta and Prof. Jukka Lehto for their valuable comments and corrections that helped me in improving the quality of the thesis. In addition, I thank Mr. Peter Jones for revising English language in some of the publications included in the thesis.

I am highly grateful to Ms. Anne Hyrkkänen for skillful assistance with the experimental and analytical work. Furthermore, I thank her for genuine support and interest in this study by discussing and helping me to solve problems also out of the office hours. In addition, I want to give many thanks to Mr. Markku Korhola and Mr. Markku Levomäki for solving several technical problems and to Mr. Juha Lehtoaro for putting these technical solutions in practice. Moreover, I wish to thank Dr. Tuomo Sainio for many interesting discussions and help for the final stage of this project. Dr. Satu-Pia Reinikainen deserves my gratitude for collaboration and invaluable help with multivariate methods. Besides of that I want to thank her and Dr. Mari Kallioinen for many helpful discussions and support during this project. Among all the people, who have worked with me during this study, I express my special thanks to Personnel of the Laboratory of Industrial Chemistry for the inspiring atmosphere. Especially, Mr. Jouni Pakarinen and Mr. Jussi Tamminen, you both are such fabulous persons and I have received much strength and faith to get through all the obstacles that have come in front of me. I am also thankful to Mr. Marko Lahtinen from Outotec Oyj for his interest and valuable ideas in this study.

Completion of this thesis would not have been possible without all the financiers. I am indebted to Finnish Cultural Foundation, National Technology Agency (TEKES), Outokumpu Oyj Foundation and the Research Foundation of Lappeenranta University of Technology for their funding and financial support.

Words fail me when I try to thank all my friends. To my friend Dr. Heli Sissonen I want to address special thanks for support and valuable advises during finishing of this thesis. Thanks for all of you that have understood that this kind of project needs very much time and much too often this time has been out of our common time. I am in a very lucky position to have such a large circle of trusted friends who have time to impart me strength and support if I just need. You all are very important to me.

I express my deepest gratitude to my dear parents, Tuula and Jukka Sirola, as well as my sisters Outi Kavasmaa and Lilli Sirola in all the paths I have taken during the past years. Especially, the keen interest of my father towards this study has given me strong motivation to go on and it is to pleasure to tell him that this work is finally done. My mother and father, no one can wish better place to grow, higher support and better advices than you have given me. I shall be always extremely thankful to you for that!

Markku Laatikainen, I cannot find words to tell you, how happy I am that our roads have met also in private life. Besides that, you have been the most important co-worker for me, you have also shown me how fantastic life can be if you have right person by your side. You are the light of my life and I can never say too much to you how much I love you.

Writing this dissertation has required lot of emotional, practical, theoretical and financial help from others. It is impossible to name all these people here, but it does not mean that I would not appreciate their assistance and contribution. I have started the dissertation process in 2004 but I was unable to work for nearly a year in 2006 and 2007 because of unfortunate injuries. Thus, I give warm thanks to all of you who were with me during these heavy times. Without your support and encouragement, this thesis would be never finished.

Lappeenranta, November 26, 2009

Katri Sirola

LIST OF PUBLICATIONS

This thesis is mainly based on the following five publications, which are referred to by the Roman numerals in the text.

I M. Laatikainen, K. Sirola and E. Paatero, Binding of Transition Metals by Soluble and Silica-Bound Branched Poly(ethyleneimine). Part I: Competitive Binding Equilibria, Colloids and Surfaces A: Physicochemical Engineering Aspects, 296 (2007) 191-205.

II K. Sirola, M. Laatikainen and E. Paatero, Binding of Transition Metals by Soluble and Silica-Bound Branched Poly(ethyleneimine). Part II: Binding Kinetics in Silica-Bound BPEI, Colloids and Surfaces A: Physicochemical Engineering Aspects, 296 (2007) 158-166.

III K. Sirola, M. Laatikainen, M. Lahtinen and E. Paatero, Removal of Copper and Nickel from Concentrated $ZnSO_4$-solutions with Silica-Supported Chelating Adsorbents, Separation and Purification Technology, 64 (2008) 88-100.

IV K. Sirola, M. Laatikainen and E. Paatero, Binding of Copper and Nickel in Silica-Supported 2-(Aminomethyl)Pyridine at Elevated Temperatures. Part I: Binding Equilibria, Reactive and Functional Polymers, (In Press)

V K. Sirola, M. Laatikainen and E. Paatero, Binding of Copper and Nickel in Silica-Supported 2-(Aminomethyl)Pyridine at Elevated Temperatures. Part II: Binding Dynamics, Reactive and Functional Polymers, (In Press)

Katri Sirola's contribution in the appended publications:

I Participation in the experimental work. Interpretation and correlation of the results together with co-authors.

II Design and supervision of the experimental work. Interpretation and correlation of the results together with co-authors, except for the model development. Preparation of the manuscript.

III As in Publication II.

IV Planning and supervision of the experimental work. Construction of the experimental setup. Interpretation and correlation of the results with the co-authors. Preparation of the manuscript.

V As in Publication IV.

CONTENTS

NOMENCLATURE

Symbols

[i]	activity of i, mol/L
D_p	pore diffusion coefficient, m^2/s
E	potential, V
E^0	standard reduction potential, V
F	Faraday constant, C/mol
G	Gibb's free energy, J/mol
H	enthalpy, J/mol
K_sp	solubility product, L/mol
K	stability constant, L/mol
K_w	ionic product of water, mol^2/L^2
N	number of components
N_L	coordination number, -
R	gas constant, J/Kmol
S	entropy, J/Kmol
T	temperature, K or $^\mathrm{o}$C
x	mole fraction of the ligand, -
β	overall stability constant, L/mol
ε_p	intra-particle porosity, -
η	current efficiency, -
ρ_s	density, kg/L
r, s, v, y, z	valence, -

Abbreviations

A, B, Me, Ne	metal cation
AMP	2-(aminomethyl)pyridine (should not be confused with (aminomethyl)phosphosphinate ligand)
AP	aminophosphonate chelating resin
aq	aqueous
BPEI	branched poly(ethyleneimine)
BPY	2,2-bipyridyl
BV	bed volume
CuWRAM	silica-supported commercial AMP adsorbent by Purity Systems Inc., USA
Dowex 4195	PS-DVB-supported commercial PMA adsorbent by Dow Chemicals
En	ethylenediamine
H	proton
i	component
IDA	iminodiacetic acid
L	ligand
LFT	ligand field theory
LFSE	ligand field stabilization energy
PHEN	1,10-phenanthroline
PMA	bis-(2-pyridylmethyl)amine
PS-DVB	polystyrene-divinylbenzene copolymer

SMB	simulated moving bed
WP-1	silica-supported commercial BPEI adsorbent by Purity Systems Inc., USA

Summary of terms

Bidentate ligand. Chelating ligand with two donor atoms.

Capacity. The amount adsorbed per unit weight of the adsorbent in the free base form.

Chelate. A metal complex, where the central atom is coordinated to several atoms of the ligand molecule

Chelating adsorbent. The functional groups are neutral ligands, which form charged complexes with metal cations and anions are co-adsorbed as counter-ions.

Chelating ion exchanger. The functional groups are charged and the metal cations act at the same time as central atoms and as counter-ions.

Coordination number. The number of donor atoms bound to the central atom.

Donor atom. Atom (N, O etc.) in the ligand molecule sharing electrons with the metal. Acts as a Lewis base.

Hydrometallurgy. A process where metals are produced from ore using aqueous solutions.

Ligand field theory. Treats the metal-ligand interaction as bonding, orbital arrangement and other characteristic of coordination complexes and depends upon considering the overlap between the d-orbitals on the metals and the ligand donor orbitals. [1]

Solvent extraction. Metals are separated from aqueous solutions using organic extractants which can be divided in four groups: cation exchange extractants, anion exchange extractants, solvating extractants and chelating extractants. [2]

Solvent impregnated resin. Solvent extractant is impregnated in solid support. Can be classified into two basic types: 1. Solvent-impregnated resins prepared by adsorption of an liquid extractant on polymer supports; and 2. Resins with liquid extractant encarcerated within polymer matrix during polymerization (TVEX and Levextrel resins). [3]

1. INTRODUCTION

Hydrometallurgical process solutions normally contain low concentrations of impurity metals which must be removed before the final product recovery step. Use of chelating adsorbents and ion exchange resins provides an alternative for conventional methods for removal of these impurities. These chelating separation materials contain donor atoms, which coordinate with metals to form various complex structures depending on the properties of the chelating ligands and metals. This complex formation property is the main reason for the high selectivity of chelating separation materials towards transition metals.

This thesis focuses on weakly basic silica-supported chelating adsorbents and their use in a hydrometallurgical application, in which copper and nickel are removed selectively from a concentrated $ZnSO_4$ solution. Although use of chelating adsorbents in hydrometallurgical applications has been widely studied during last 40 years, binding mechanism and stoichiometry are still uncertain. Moreover, the effect of temperature on the complex formation chemistry is not fully elucidated, especially at temperatures above 40 ^{o}C. Thus, the factors affecting removal of small concentrations of copper and nickel from concentrated $ZnSO_4$ solution were studied in detail. In particular, the effect of temperature on complex formation in chelating adsorbents and their behavior in dynamic column separation was investigated. The following introduction gives on overview of the commonly used hydrometallurgical separation methods and reviews the basic principles governing metal binding in chelating materials. Moreover, only equilibrium phenomena are described here in detail, because binding rates are usually controlled by diffusion and the present case does not especially differ from those found in standard textbooks [4-5].

1.1. Hydrometallurgical separation processes

Hydrometallurgy simply means a process where metals are produced from raw material (ores, metal concentrates, calcined concentrates etc.) using aqueous solutions. Hydrometallurgical methods cannot always compete economically with pyrometallurgical processes because of much slower reaction rates and thus slower productivity. It may be said, however, that such processes have played an important role in development of the present-day metal-refining industry striving for more clean technology. If pyrometallurgy usually is suitable for recovery of high-grade ores, hydrometallurgical processes offer possibility for the recovery of low-grade, complex and small-body ores. Although hydrometallurgical processes not always are the most cost-effective alternatives, they are of high priority in development and research less polluting production.

In a typical hydrometallurgical process, valuable constituents are first leached from the raw material, purified from impurities using various solution purification methods and finally the target metals are recovered by electrowinning. Representative hydrometallurgical separation and purification processes include chemical precipitation, cementation, solvent extraction, ion exchange and adsorption. The methods are briefly described below and their advantages, disadvantages and applications are compared in Table 1. Also membrane separation and crystallization can be used in some specific cases but their industrial use is limited to pre-treatment stage for other separation techniques [6-9].

1.1.1. Chemical precipitation

Chemical precipitation is old and important hydrometallurgical separation method, which means removal of various impurities by means of additives which chemically react with the impurities and form solid precipitates [10]. In hydrometallurgical applications chemical precipitation can be used for instance for separations of cobalt and nickel or iron and zinc [11-12].

Metal ions are usually precipitated from the solution as hydroxides, carbonates or sulfides [10, 13]. Dissolution of the sparsely soluble salts in water can be described as shown in Eq. 1 for a hydroxide of a divalent metal.

$$\mathrm{Me(OH)_2}(s) + \mathrm{nH_2O} \rightleftarrows \mathrm{Me^{2+}(H_2O)_6}(aq) + \mathrm{2OH^-}(aq) + \mathrm{(n\text{-}6)H_2O} \tag{1}$$

The solubility product K_{sp} is defined by Eq. 2, where the square brackets indicate activity.

$$K_{\mathrm{sp}} = [\mathrm{Me^{2+}}][\mathrm{OH^-}]^2 \tag{2}$$

The solubility characteristics can be illustrated using precipitation diagrams, in which metal ion concentration in solution is plotted against solution pH [13]. As an example, precipitation diagram for metal hydroxides can be calculated from Eq. 3, which relates metal concentration to pH for a given solubility product K_{sp}. K_{w} is the apparent ionic product of water.

$$\log[\mathrm{Me^{2+}}] = \log K_{\mathrm{sp}} - 2(\log K_{\mathrm{w}} + \mathrm{pH}) \tag{3}$$

Copper, nickel, cobalt and cadmium separation by hydroxide precipitation is discussed in Section 1.3.1 and the precipitation diagram for the common metal hydroxides is shown in Fig. 9 (p. 33). On the left-hand side of the equilibrium lines, metal ions dissolve in the solution while stable solid phase is present on the right-hand side of the lines [13].

1.1.2. Cementation

Cementation is a special precipitation method, which is based on the difference in reduction potentials and the impurity metals can be precipitated on a more electronegative metal surface [14]. Cementation efficiency depends on differences in reduction potentials; the higher is the difference, the higher is the amount of the precipitated metal. Cementation process consists of several steps but in most cases cementation follows first-order kinetics and it is controlled by diffusion [15].

The cementation reaction can be described by Eq. 4.

$$\mathrm{Me}^{z+} + \frac{z}{y}\mathrm{Ne}^0 \rightleftarrows \frac{z}{y}\mathrm{Ne}^{y+} + \mathrm{Me}^0 \tag{4}$$

Me^{z+} and Ne^{y+} are the ionic forms of the impurity metal and the cementing metal, and Me^0 and Ne^0 are metallic forms of the same [14]. This reaction is composed of oxidation of Ne and reduction of Me, and cementation equilibrium can be represented by the Nernst equations written for each half-cell reaction (Eq. 5). E is potential, E^0_{Me} is a standard reduction potential of metal Me, R is the gas constant, T is the absolute temperature, n is number of electrons transferred and F is the Faraday constant [14].

$$E = E^0_{Me} - \frac{RT}{nF}\ln[\mathrm{Me}] \tag{5}$$

Cementation has been extensively studied as a hydrometallurgical separation method and the effects of operation conditions (temperature, pH, concentrations) are well understood [14-16]. Most common applications of cementation separation processes include copper removal with broken iron [16], copper, nickel, cobalt and cadmium removal from concentrated zinc sulfate solution using zinc powder [15-22], gold removal from copper with zinc powder [14] and purification of lead, cadmium, nickel and cobalt from ammoniacal zinc leaching solution with zinc powder [23].

Copper, nickel, cobalt and cadmium separation by cementation from concentrated $ZnSO_4$ solution is discussed in Section 1.3.1 and the standard reduction potentials of different metals present in the zinc process solution are shown in Table 8 (p. 32).

1.1.3. Solvent extraction

Solvent extraction is hydrometallurgical separation method, in which metals are separated from aqueous solutions using organic extractants. The aqueous metal solution is first dispersed with organic phase containing the active extractant. Active extractant reacts with the desired metal and transfers it into the organic phase. After separation of the phases, the organic phase loaded with the desired metal is mixed with a stripping solution. This transfers the loaded metal back to aqueous phase. Stripped organic phase is recycled back to extraction and aqueous solution with desired metal goes to final metal recovery.

The extractants can be divided in four groups: cation exchange extractants, anion exchange extractants, solvating extractants and chelating extractants. Typical cation exchange extractants are carboxylic and alkyl phosphonic acids. Tertiary alkyl amines are examples of anion exchange extractants. Solvating extractants are oxygen–containing organic compounds and the metal binding mechanism is based on replacing hydration water around the metal ions. Ethers, esters, alcohols, ketones and alkyl-phosphate esters are examples of solvating extractants [2]. Chelating extractants form one of the most important groups of extractants because of the high selectivity for transition metals relative to alkali and alkaline earth metals. Chelating extractants consist of chelating ligands, which have one or more donor atoms in the structure. Hydroxyoximes and β-diketones are examples of extractants which are selective for copper and nickel. A more detailed discussion on chelating mechanism and coordination chemistry is given in connection of solid chelating separation materials (Section 1.2).

Ritcey [24] has extensively reviewed solvent extraction applications in hydrometallurgy for primary metal recovery and for secondary or environmental processing. Solvent extraction is generally adopted for the recovery of high metal ion concentrations from aqueous solutions [25]. In a conventional solvent extraction, limiting factors are the ratio of solvent to feed and the distribution ratio of the solute between the phases, which mean that a large amount of solvent is necessary [26]. Liquid membranes (LM), liquid surfactant membranes (LSM) and supported liquid membranes (SLM) have been studied as more economical alternatives. Because of stability problems of a liquid membrane emulsion, colloidal solids incorporation and lower selectivity, these methods have not displaced conventional solvent extraction. Solvent extraction as a separation method for the concentrated zinc sulfate solution is further discussed in Section 1.3.1.

1.1.4. Adsorption and ion exchange

In ion exchange ions are separated from solution by means of solid inorganic oxides or organic ion exchange resins carrying fixed negative or positive charge. Equivalent amount of ions are exchanged from solution and attached to solid particles. Ideal ion exchange reaction is stoichiometric and reversible but strong chemical interactions can change stoichiometry and in some cases even make reaction irreversible. Organic ion exchange resins are divided into cationic, anionic and chelating resins meaning that cationic, anionic or chelating organic ligands have been attached onto surface of the solid support.

Ion exchange selectivity for two different metal cations, A and B can be illustrated with selectivity coefficient $K_{\mathrm{A/B}}$ (Eq. 6), in which overbar indicates metal concentrations in the resin [27].

$$|z_B|\,\bar{A}^{z_A} + |z_A|\,B^{z_B} \rightleftarrows |z_B|\,\bar{B}^{z_B} + |z_A|\,A^{z_A}$$

$$K_{\mathrm{A/B}} = \frac{[\bar{A}]^{|z_B|}[B]^{|z_A|}}{[\bar{B}]^{|z_A|}[A]^{|z_B|}} \tag{6}$$

If the selectivity of the ion exchanger or adsorbent is high, it usually means slow ion exchange or binding kinetics [28]. The overall rate is controlled by boundary layer diffusion (external mass transfer), intraparticle diffusion (mass transfer through the pores), by the rate of ion exchange or adsorption reaction, or by a combination of them [27, 29]. In most cases, the rate determining steps are external or intraparticle diffusion [27, 29]. In this study, conventional mass transport theories are used to explain the dynamic behavior of chelating adsorbents as will be shown in Papers [II] and [V].

In adsorption, the phase equilibrium can be described with different well-known adsorption models, such as Langmuir or Freundlich isotherms. In this study, a non-ideal competitive adsorption (NICA) model is used and details can be found in Paper I.

Ion exchange is executed in fixed-bed columns. Processes are nowadays continuous multicolumn systems; columns in series are used when longer contact time is needed and columns in parallel are used when longer contact surface area is needed. Simulated moving bed (SMB) process is one of the first truly continuous separation systems. Sequential simulated moving bed process is a modification of the SMB-process, where feed, elution and liquid circulation form process cycles, which are performed in sequences.

In hydrometallurgy, ordinary ion exchange resins are mainly used in recovery of valuable metals from dilute solutions and in purification of wastewaters [25, 27, 30-35]. High selectivity is often the key factor and chelating ion exchangers or adsorbents are the most promising alternative in such processes. The chelating separation materials are discussed in more detail in Section 1.2. In this thesis, the proposed adsorption process is considered as partial substitute for the conventional solution purification step of $ZnSO_4$ process solution and this case is discussed in Section 1.3.1.

Table 1. The main features of chemical precipitation, cementation, solvent extraction and ion exchange/adsorption in hydrometallurgy.

	Chemical Precipitation	
Advantages	**Disadvantages**	**Applications**
• Well-established technology • Inexpensive chemicals • Useful in a wide concentration range	• Sensitive to precipitation conditions, e.g. pH, redox • Waste problems, e.g. gypsum, jarosite • Dust	• Recovery of first row transition metals • Treatment of waste solutions
	Cementation	
• Simple and economical method for dilute solutions • Nearly stoichiometric reaction → good efficiency • More valuable metal can be separated with less valuable metal	• Back-dissolution by oxygen • Reduction of other cations at high oxidation degree to lower oxidation degrees • Hydrogen evolution at acidic conditions	• Removal of copper with broken scrap iron powder • Removal of copper, nickel, cobalt, cadmium etc. from zinc sulfate solutions with zinc powder
	Solvent Extraction	
• Established technology with long industrial experience • Suitable in many applications because of large variety of extractants • Fast and selective • Economical also for high flow rates	• Volatile and flammable organic solvents increase environmental and safety risks • Large amounts of solvents and complexing agents are needed • Incomplete phase separation → chemical losses	• Copper, cobalt, nickel, zinc, uranium extraction from primary sources • Removal of impurity metals in solution purification, e.g. calcium, iron, manganese • Recovery of secondary metals, e.g. germanium, arsenic, indium, rhenium, molybdenum,
	Ion Exchange and Adsorption	
• Highly selective and eco-friendly • Can be used at very low metal concentrations • Closed and automated operation	• Selectivite chelating separation materials are expensive • Metal capacity is relatively low (usually < 3 mequiv_l/g) • May degrade by oxidation, mechanical attrition, temperature or osmotic shock • Often slow uptake kinetics	• Recovery of uranium • Purification of electrolytes by removing e.g. copper, nickel, cobalt, zinc, iron, arsenic, chromium • Recovery of noble metals

1.2. Chelating separation materials

Chelating separation materials considered in this thesis consists of organic chelating ligands supported on solid supports. These materials include both ion exchange resins and adsorbents which contain chelating ligands as a functional group. In literature, the definitions are somewhat confusing and in many cases all such materials are called chelating ion exchangers even if some of them are adsorbents. The distinction between the two types is clarified in Fig. 2. Iminodiacetic acid (IDA) (Fig 2A) and bis-(2-pyridylmethyl)amine (PMA) (Fig. 2B) are good examples of functional groups of a chelating ion exchange resin and adsorbent, respectively. In chelating ion exchangers the ligands are charged and the metal cations act at the same time as central atoms and as counter-ions. In the case of chelating adsorbents, the neutral ligands form charged chelates with metals and anions are co-adsorbed as counter-ions.

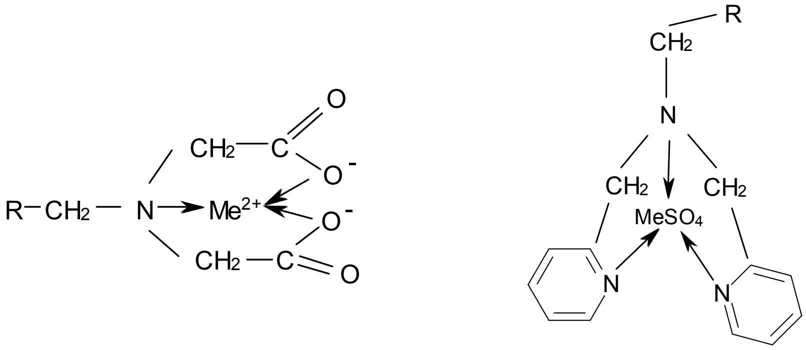

(A) (B)

Figure 2. Chelating ion exchange resin with iminodiacetic acid (IDA) groups (A) and chelating adsorbent with bis-2-(pyridylmethyl)amine (PMA) groups (B). R means the solid support.

Similar ligands can be also used as functional groups of chelating extractants used in solvent extraction. The same principles thus apply for both solid chelating separation materials and organic extractants, although the effect of organic solvent can be in some cases significant [36]. Therefore, basic factors affecting complex formation between transition metals and chelating ligands can be discussed using soluble ligands as model compounds.

1.2.1. Chelate formation, coordination numbers and geometric configurations

Chelating ligands act as donors of electrons and form coordinative bonds to a metal cation called as the central atom. When a molecule has two or more donor atoms in the structure and it participates in a ring-closure reaction, it is called chelating ligand [37]. Electron acceptor, the metal atom, acts as a Lewis acid and electron donor, the chelating ligand, acts as a Lewis base. Ethylenediamine (En) is a good example of chelating ligands. One En can form two bonds with, for example, a Ni^{2+} ion. Moreover, the remaining 4 water molecules around the Ni^{2+} ion can be replaced by two additional ligands as shown in Fig. 3.

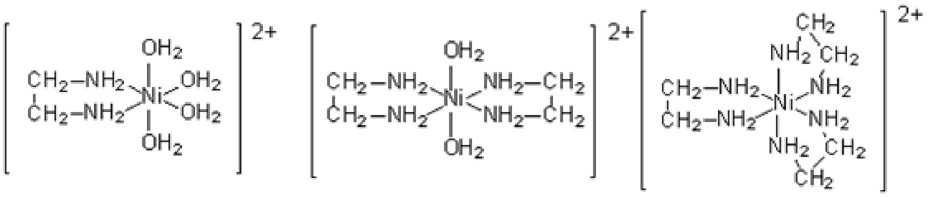

Figure 3. Complex structures between Ni^{2+} ion and ethylenediamine [38].

Fig. 3 also illustrates the general step-wise formation mechanism, which can be described by Eq. 7. Me is the metal ion, L is ligand, $K_{\mathrm{Me},1}$, $K_{\mathrm{Me},2}$…$K_{\mathrm{Me},,\mathrm{N}}$ are the step-wise stability constants and β is the overall stability constant.

$$\begin{array}{ll}
\mathrm{Me} + \mathrm{L} = \mathrm{MeL} & K_1 = \dfrac{[\mathrm{MeL}]}{[\mathrm{Me}][\mathrm{L}]} \\
\mathrm{MeL} + \mathrm{L} = \mathrm{MeL}_2 & K_2 = \dfrac{[\mathrm{MeL}_2]}{[\mathrm{Me}][\mathrm{L}]} \\
\mathrm{MeL}_2 + \mathrm{L} = \mathrm{MeL}_3 & K_3 = \dfrac{[\mathrm{MeL}_3]}{[\mathrm{Me}_2][\mathrm{L}]} \\
\cdot & \cdot \\
\cdot & \cdot \\
\cdot & \cdot \\
\mathrm{MeL}_{\mathrm{N-1}} + \mathrm{L} = \mathrm{MeL}_{\mathrm{N}} & K_{\mathrm{N}} = \dfrac{[\mathrm{MeL}_{\mathrm{N}}]}{[\mathrm{MeL}_{\mathrm{N-1}}][\mathrm{L}]} \\
\\
\mathit{Overall}:\ \beta = K_1 K_2 K_3 \ldots K_{\mathrm{N}} &
\end{array} \tag{7}$$

It is also well-known that complex formation constants for multidentate ligands are much larger than for unidentate ligands. This has been explained with chelate effect which is a result of a different number of water molecules released from the first coordination sphere (Eq. 8) [39-41]

$$\mathrm{Me(H_2O)_6} + \mathrm{L} \rightleftarrows \mathrm{MeL(H_2O)_5} + \mathrm{H_2O} \tag{8}$$

The number of donor atoms bound to the central atom determines the coordination number of the metal complex. In general, the coordination numbers of different metals range from 2 to 9, of which 4 and 6 are the most common [42]. Furthermore, chelates with each coordination number can form various coordination geometries [43]. Some coordination geometrics with coordination numbers of 4-6 are shown in Fig. 4 [42-44]. Most important structures for this study are octahedral and distorted octahedral. The square planar geometry can be considered as an extreme case of distortion, where the two axial ligands are removed.

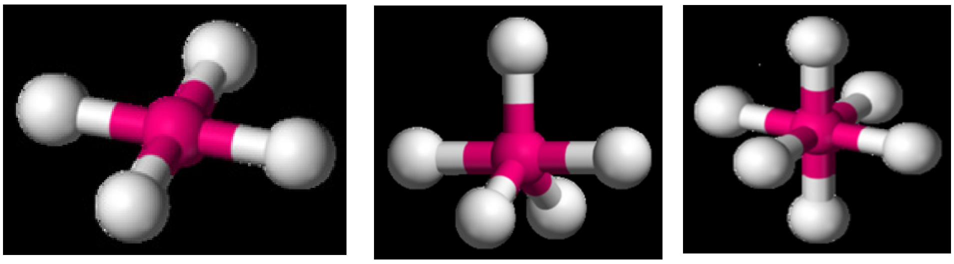

Square planar (4) Trigonal bipyramidal (5) Octahedral (6)

Figure 4. Different coordination geometries for coordination numbers 4-6 [44].

1.2.2. Interactions between metal ions and chelating ligands

The interactions between metals and chelating separation materials depend on properties of the metal, the solution and the ligand group [45]. Metal-ligand affinity is the most important factor in explaining the selectivity properties of different chelating materials and metals. In this work, main interest is in bidentate nitrogen ligands and most of the examples given below are for ethylenediamine (En), 2-(aminomethyl)pyridine (AMP), 1,10-phenanthroline (PHEN) and 2,2-bipyridyl (BPY). The chemical structures are shown in Fig. 5. Some results are also shown for a tridentate nitrogen ligand bis-(2-pyridylmethyl)amine (PMA), which is widely used in hydrometallurgical industrial applications (Section 1.2.4.). The chemical structure of PMA was shown in Fig. 2. It should be noted that the abbreviation AMP is sometimes used for the (aminomethyl)phosphonate ligand in ion-exchangers.

Ethylenediamine (En) 2-(aminomethyl)pyridine (AMP) 1-10-phenanthroline (PHEN) 2,2-bipyridyl (BPY)

Figure 5. The chemical structures of chelating ligands.

All the ligands shown in Fig. 5 contain two nitrogen atoms separated by two carbon atoms and the basicity decreases from left to right.

There are several theories to explain the metal-ligand interactions and many books have been written about this topic [37, 42-43, 46]. The metal-ligand affinities can be described qualitatively using the theory of hard and soft acids and bases [47-49]. A more quantitative approach to predict complex stabilities is given by the ligand field theory [42, 46]. Moreover, the kinetic theory of metal-ligand complexes [50-51] gives insight into various elementary steps involved in the process.

Pearson Theory

According to theory of the Pearson [47-49], metal affinity towards a given ligand is explained by acid-base interactions and the Lewis acids (electron acceptors) and bases (electron donors) can be divided into hard and soft acids and bases. Soft acids form stronger bonds with soft bases, whereas hard acids prefer hard bases. Hardness is associated with small ionic radius, high oxidation state, low polarizability and high electronegativity, whereas softness is associated with large atomic/ionic radius, low or zero oxidation state, high polarizability and low electronegativity [47-49]. Typical hard and soft acids and bases are shown in Table 2 [52]. However, there are some borderline cases, which have intermediate values of acidity or basicity [52], and the association is not clear with these borderline compounds.

Table 2. Hard and soft acids and bases [data from Ref. 52].

Acids			Bases		
Hard acids	Soft acids	Borderline acids	Hard bases	Soft bases	Borderline bases
H^+	Cu^+	Mn^{2+}	OH^-	H^-	C_6H_7N
Li^+	Ag^+	Fe^{2+}	RH^-	RS^-	C_5H_5N
Na^+	Au^+	Co^{2+}	F^-	I^-	N_2
K^+	Hg^+	Ni^{2+}	Cl^-	PR_3	N_3^-
Mg^+	Cs^+	Cu^{2+}	NH_3	SCN^-	Br
Ca^{2+}	Pd^{2+}	Zn^{2+}	CH_3COO^-	CO	NO_3^-
Sn^{2+}	Cd^{2+}	Pb^{2+}	CO_3^{2-}	C_6H_6	SO_4^{2-}
Al^{3+}	Pt^{2+}		N_2H_4		
La^{3+}	Hg^{2+}				
Cr^{3+}					
Co^{3+}					
Fe^{3+}					
As^{3+}					

Ligand Field Theory

First-row transition metals studied in this thesis (Mn^{2+}, Fe^{2+}, Co^{2+}, Ni^{2+}, Cu^{2+} and Zn^{2+}) have partially filled *d* electron shells, which affect their complex formation [42]. All first-row transition metals can form high-spin octahedral metal complexes and the general stability sequence can be written as $Mn^{2+} < Fe^{2+} < Co^{2+} < Ni^{2+} < Cu^{2+} > Zn^{2+}$. This is called the Irving-Williams series [53]. These metals are also defined as borderline acids according to Pearson theory [47-49]. Irving-Williams series have been found to hold for a wide variety of ligands [53-54] and the stability order has been explained with the ligand field theory (LFT). More specifically, the ligand field stabilization energy (LFSE) varies with electron occupancy in the *d* shell [55]. In Fig. 6 are shown the first step-wise stability constants ($\log K_1$) for ethylenediamine (En) complexes of first row transition metals [55]. As can be seen, stability minima are observed at d^0, d^5 and d^{10} and coordination complexes with these metal ions are not very stable [42, 55]. LFSE calculations predict, however, that Ni^{2+} should form more stable complexes than Cu^{2+} (Fig. 2), although Cu^{2+} complexes are usually more stable [55]. This is due to Jahn-Teller effect, which means that octahedral copper complexes are distorted, which results in extra stability [55]. Because of the distortion in the copper complexes, the two axial bonds are shorter than in regular octahedral complexes [55].

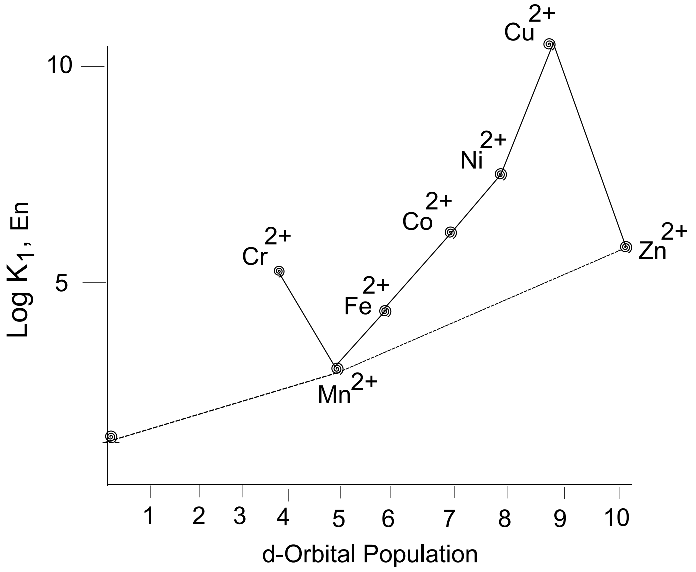

Figure 6. First step-wise stability constants (logK_1) of ethylenediamine (En) for first-row transition metals [data from Ref. 55].

1,10-phenanthroline (PHEN) and 2,2-bipyridyl (BPY) are examples of ligands, which form less stable octahedral complexes with Cu^{2+} ions than with Ni^{2+} ions [55]. Garcia-Espana et al. [56] have studied formation of the 1:1, 1:2 and 1:3 complexes of Mn^{2+}, Fe^{2+}, Co^{2+}, Ni^{2+}, Cu^{2+} and Zn^{2+} with EN, AMP and BPY at 25 °C and ionic strength of 0.1 M. Results are shown in Fig. 7 and it is clearly seen that the 1:1 complexes of these ligands follow the Irving-Williams series. In the case of PHEN and also BPY [57], the 1:2 complex with Cu^{2+} has, however, lower stability than with Ni^{2+} (Fig. 7B).

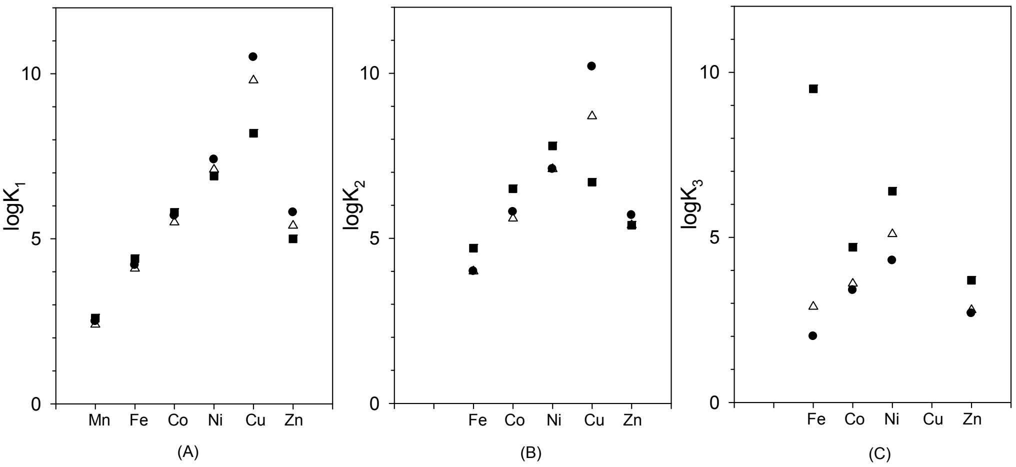

Figure 7. Stability constants of the 1:1 (A), 1:2 (B) and 1:3 (C) complexes of Mn^{2+}, Fe^{2+}, Co^{2+}, Ni^{2+}, Cu^{2+} and Zn^{2+} with En (filled circles), AMP (open triangles) and BPY (filled squares) at 25 °C. $I = 0.1$ M [data from Ref. 56].

Kinetic Theory

According to the kinetic theory [50], the rate determining step in complex formation reactions is a process, in which the first water molecule of the metal ion's innermost hydration shell is substituted by the ligand. The original theory of complex formation kinetics of metals in aqueous solutions was presented by Eigen and Tamm [50]. They considered complexation between metal and ligands as a three-step substitution process, in which the hydrated reactants first approach each other with formation of an encounter complex. In the first step outer-sphere complex between hydrated metal ion $Me(H_2O)_6$ and ligand L is formed. This step is fast, essentially instantaneous equilibrium. In the second step the first coordinating Lewis base site of the ligand replaces one coordinated water molecule. This step is rate-determining and controlled by the water-exchange rate of the *aquo* complex [58]. Finally, substitution of part of the innermost coordination sphere's water molecules by the ligand results in the formation of the inner-sphere complex MeL. First complexation step of the metal ion, Me, with the ligand, L, in aqueous solution is thus illustrated by Eq. 9. [51, 58-59]:

$$\mathrm{Me(H_2O)_6} + \mathrm{L} \rightleftarrows \mathrm{Me(H_2O)_6} \cdots \mathrm{L} \rightleftarrows \mathrm{MeL(H_2O)_5} + \mathrm{H_2O} \qquad (9)$$

Water exchange rate constants k for copper, nickel, cobalt, zinc and cadmium ions having different electron configurations are shown in Fig. 8. The water exchange is fast in the case of copper and its first-order rate constants is almost 10^{10} s^{-1} whereas the water exchange in nickel is significantly slower and the rate constant is about 10^5 s^{-1} [1].

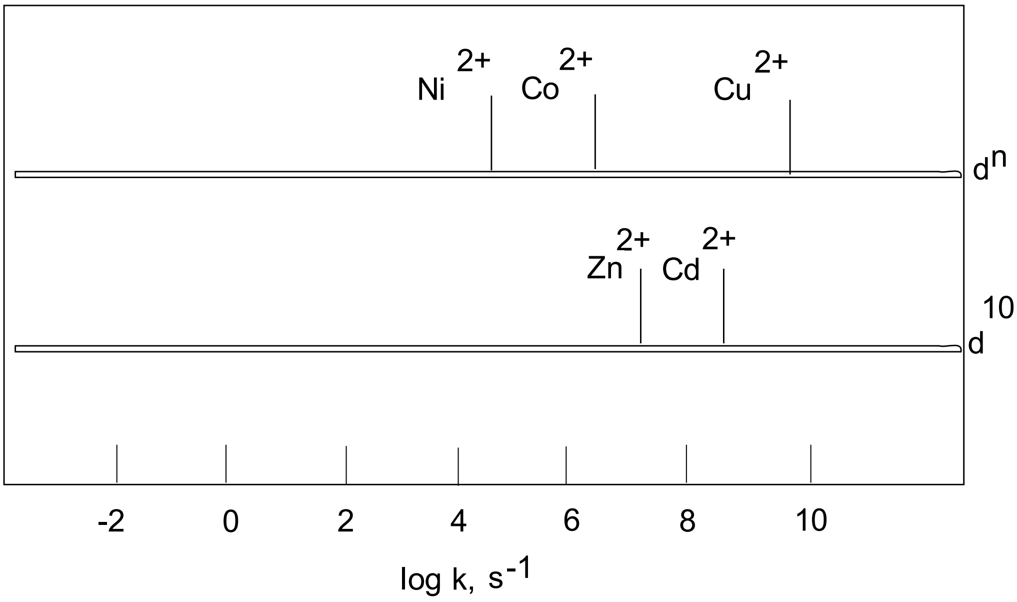

Figure 8. Comparison of water exchange rate constants for various metal *aquo* complexes [data from Ref. 1].

The coordination kinetics between metal-ions and chelating ligands becomes very complicated in slightly acidic aqueous solutions [58]. For instance, Fabian and Diebler [60], Diebler [51], Taylor [61] and Grant [62] have studied the kinetics of formation and dissociation of the En- and BPY-complexes of Cu^{2+} and Ni^{2+} both with unprotonated and partly protonated ligands. The formation rate constants are shown in Table 3 [51, 60-62]. The data show that complex formation of both ligands with copper is considerably faster than with nickel. As was explained above, this is due to slow water exchange rate of nickel (see Fig. 8). Other very interesting observation was that complex formation rate decreases dramatically, when the ligands become partly protonated.

Table 3. Formation rate constants of unprotonated and protonated ethylenediamine and bipyridyl ligands with Cu^{2+} and Ni^{2+} ions.

Formation rate constants, L mol^{-1}s^{-1}						
Metal	**En**	**EnH**	**$Me(H_2O)_4(BPY)^{2+}$**	**$Me(H_2O)_2(BPY)_2^{2+}$**	**$Me(H_2O)_4(BPY)^{2+}H$**	**$Me(H_2O)_2(PBY)_2^{2+}H$**
Cu^{2+}	$3.8\cdot10^9$ (a)	$1.4\cdot10^5$ (a)	$5.0\cdot10^7$ (b)	$1.5\cdot10^9$ (b)	$2.6\cdot10^5$ (b)	$2.7\cdot10^6$ (b)
Ni^{2+}	$3.5\cdot10^5$ (c)	$1.8\cdot10^2$ (c)	$1.99\cdot10^5$ (b)	$1.32\cdot10^5$ (d)		

a = Ref. Diebler [51]
b = Ref. Fabian and Diebler [60]
c = Ref. Taylor et al. [61]
d = Ref. Grant et al. [62]

Generally, the complex formation kinetics is sufficiently fast and it rarely is the rate determining step in the separation applications with solid chelating separation materials. This point is discussed in detail in Paper [II].

1.2.3. Effect of operating conditions on chelate formation

In the case of chelating separation materials, operating conditions, including acid concentration (pH), ionic strength, and temperature, have strong influence on the adsorption equilibrium.

pH

Most of the well-known chelating ligands exist as an equilibrium mixture of both protonated and unprotonated forms and metal ions compete with hydrogen ions for the available donor atoms. Competitive binding equilibria of proton and metal cation, Me, is illustrated in Eq. 10.

$$\begin{aligned}
&L + H^+ \overset{K_{\mathrm{LH}}}{\rightleftarrows} LH^+ \\
&L + xH^+ \overset{K_{\mathrm{LH}x}}{\rightleftarrows} LH_x^{x+} \\
&Me^{2+} + L \overset{K_{\mathrm{MeL}}}{\rightleftarrows} MeL^{2+} \\
&Me^{2+} + LH^+ \overset{K_{\mathrm{MeLH}}}{\rightleftarrows} MeL^{2+} + H^+ \\
&Me^{2+} + LH_x^{x+} \overset{K_{\mathrm{MeLH_x}}}{\rightleftarrows} MeL^{2+} + xH^+ \\
&\qquad\quad \vdots \qquad\qquad\qquad \vdots
\end{aligned} \tag{10}$$

Displacement of hydrogen ions by a metal ion from the protonated form of the ligand and, on the other hand, displacement of metal ions by hydrogen ions depends on the basicity of the ligand. If the ligand is strongly basic (K_{HL} large), displacement of metals can be achieved with quite dilute acid. At the same time, displacement of protons from the ligands with metal ions is difficult and ligands have to be used in unprotonated form. In this case metal precipitation may become a problem because of high proton affinity of the ligand (see Section 3.2.3).

Generally the effect of pH to the characteristics of soluble chelating ligands and solid chelating separation materials is described with potentiometric pH titration curves. The same principles of the pH titration curves are valid in the case of chelating separation materials as in the case of ordinary ion exchange resins. The potentiometric pH titration curve can be thus used to evaluate the number of functional groups and dissociation constants. However, a correct interpretation of potentiometric pH titration curves can be given only when the mechanism is well understood. [27] Effect of pH on characteristics of soluble and silica-supported BPEI and AMP was studied in detail in this thesis and the results are discussed in Papers [I, III, IV].

Ionic strength

Ionic strength has a strong influence on the acid/base properties of ligands and on the complex formation. As an example, general trends observed in stability constants of divalent metal ions and some ligands are shown in Table 4. The figures indicate changes relative to values measured at ionic strength of 0.1 M, and bracketed values are estimates based on trends. [63]

Table 4. Change of stability constants of divalent metal ions with ionic strength. Values indicate changes relative to 0.1 M ionic strength and values in square brackets are based on trends [from Ref. 63].

Ligand	**Ionic strength**	**0.0**	**0.5**	**1.0**	**2.0**	**3.0**
L^-	$\log K_1$	+0.4	-0.2	-0.2	-0.1	0.0
	$\log\beta_2$	+0.6	-0.4	-0.4	-0.3	0.0
L^{2-}	$\log K_1$	+0.8	-0.4	-0.4	-0.4	[-0.3]
	$\log\beta_2$	+1.2	-0.8	-0.8	[-0.7]	[-0.5]
L^{3-}	$\log K_1$	+1.2	-0.6	-0.6	[-0.7]	[-0.6]
	$\log\beta_2$	+1.8	[-1.0]	[-1.0]	[-1.0]	[-0.9]

The increasing metal uptake can be explained by co-adsorption of the anion [64]. In this thesis, all experiments were made at high ionic strength and such effects are not important. The supporting ionic strength of the synthetic sulfate solution was 2 mol/L and the ionic strength estimated for the authentic $ZnSO_4$ process solution is about 2.5 mol/L. Consequently, activity coefficients can be assumed to be nearly constant and the effect of electrostatic interactions can be neglected.

Temperature

As discussed above, formation equilibria of chelating ligands and metals ions can be illustrated with Eq. 7, where the equilibrium constant of step n is given by K_n (n = 1-N). Temperature dependence of K_n is obtained by using the well-known thermodynamic relationship given in Eq.11. ΔG_n means the reaction Gibb's energy, ΔH_n means reaction enthalpy related to the bond energies and ΔS_n means reaction entropy, which is related to reorganization or reforming of the bonds [65]. ΔH_n and ΔS_n can be calculated from the K_n values determined at different temperatures from the linearized form of Eq. 11 (van't Hoff plot).

$$\Delta G_n = -RT \ln K_n = \Delta H_n - T\Delta S_n$$
$$\ln K_n = \frac{\Delta S_n}{R} - \frac{\Delta H_n}{RT} \qquad (11)$$

In order to illustrate the possible effects of temperature on protonation and complex formation, the literature data on transition metal complexes of En, AMP, PHEN and BPY are discussed here. The step-wise quantities $\log K_n$, ΔH_n and ΔS_n at 10-40 °C for H^+, Cu^{2+}, Ni^{2+} and Zn^{2+} are shown in Table 5.

Table 5. Values for the thermodynamic quantities logK_n, ΔH_n and ΔS_n at temperatures between 10-40 °C for H^+, Cu^{2+}, Ni^{2+} and Zn^{2+} and ethylenediamine, 2-(aminomethyl)pyridine, 1,10-phenanthroline and 2,2-bipyridyl.

Ethylenediamine [66]							
		logK_n				**ΔH_n, kJ/mol**	**ΔS_n, J/molK**
Ion	n	T = 10°C	T = 20°C	T =30°C	T =40°C	T = 10-40°C	T = 10-40°C
H^+	1	10.39	10.09	9.81	9.53	-48.1	-29
	2	7.28	7.00	6.79	6.5	-43.1	13
Cu^{2+}	1	11.01	10.67	10.36	10.06	-53.5	-21
	2	9.57	9.23	8.93	8.66	-51.4	0
Ni^{2+}	1	7.74	7.52	7.27	7.04	-39.7	-8
	2	6.44	6.32	6.11	5.89	-31.4	-13
	3	4.67	4.49	4.2	4.05	-36.4	38
Zn^{2+}	1	5.85	5.77	5.55	5.51	-20.9	-38
	2	5.13	5.06	4.89	4.76	-21.7	-21
2-(Aminomethyl)pyridine [67]							
		logK_n				**ΔH_n, kJ/mol**	**ΔS_n, J/molK**
Ion	n	T = 10°C	T = 20°C	T =30°C	T =40°C	T = 10-40°C	T = 10°C
H^+	1	9.09	8.78	8.51	8.34	-43.1	21
	2			3.1	2.8		
Cu^{2+}	1	9.9	9.64	9.45	9.17	-40.2	46
	2	8.26	7.98	7.8	7.58	-37.5	25
Ni^{2+}	1	7.49	7.23	7.09	6.86	-34.9	21
	2	6.56	6.32	6.08	5.87	-38.7	-13
	3	5.31	5.07	4.95	4.66	-35.2	-25
Zn^{2+}	1	5.53	5.41	5.17	5.04	-28.5	4
	2	4.61	4.44	4.21	4.09	-30.4	-4
	3	3.29	3.12	3.07	2.83	-24.5	-25
1,10-Phenanthroline [57]							
		logK_n	**ΔH_n, kJ/mol**	**ΔS_n, J/molK**			
Ion	n	T = 25°C	T = 20°C	T = 20°C			
H^+	1	4.9	-16.5	38			
Cu^{2+}	1	8.8^{d}	-48.9	10			
	2	6.57^{d}	-76.1	47			
	3	5^{d}	-110.4	31			
Ni^{2+}	1	8^{d}	-46.8	9			
	2	8^{d}	-85.7	34			
	3	7.9^{d}	-125.4	47			
Zn^{2+}	1	6.36	-31.4	18			
	2	5.64	-62.7	23			
	3	5.2	-80.7	60			
2,2-Bipyridyl [68]							
		ΔH_n, kJ/mol	**ΔS_n, J/molK**				
Ion	n	T = 30.3°C	T = 30.3C				
H^+	1	-16.8	-				
Cu^{2+}	1	-42.5	20				
	2	-79.5	6				
	3	-90.4	40				
Ni^{2+}	1	-37.2	10				
	2	-74.4	18				
	3	-111.6	17				
Zn^{2+}	1	-26.1	15				
	2	-49.1	26				
	3	-66.5	44				

Basicity order of the ligands is En > AMP > PHEN ≈ BPY, where En is the most basic and BPY the least. According to Table 5, first protonation step in AMP is less basic and slightly less exothermic than in the case of En. According to Garcia-Espana et al. [56], this can be explained in terms of an electron-withdrawing effect promoted by the pyridine ring, which make the protonation of AMP less exotermic. Temperature thus affects protonation of all four ligands in a similar way; binding constant of acid is decreasing with increasing temperature. In a similar way, stabilities of the Cu^{2+}, Ni^{2+} and Zn^{2+}complexes decrease when temperature increases.

In the case of chelating adsorbents, binding mechanism between metals and the functional group is qualitatively similar as discussed above for unsupported ligands. Consequently, analogous effect of temperature is expected to be present also in solid materials. These factors are surveyed in more detail in Paper [IV]. Temperature also affects significantly the uptake rates and the dynamic aspects are studied in Paper [V].

1.2.4. Chelating separation materials in hydrometallurgical applications

As discussed above, chelating ligands form easily stable complexes with transition metals and thus chelating separation materials are a reasonable choice in the removal of transition metals from hydrometallurgical solutions. During last 40 years the use of chelating separation materials in hydrometallurgical separation and purification applications has been actively studied and many specifically tailored materials have been proposed for impurity removal and purification of electrolyte solutions. The markets offer a wide selection of commercial chelating separation materials and IDA [70-74], aminophosphonate (AP) [75-77] and PMA [64, 78-85] are the examples of widely studied ligands used in chelating separation materials.

Despite the high prices of these special separation materials, the selectivity towards transition metals is so high in comparison with conventional ion exchangers, that their use also in industrial scale is warranted. IDA resin is used for instance by Queensland Nickel, in Townswille, Queensland, Australia in a lead-lag system to remove calcium and magnesium from the ammoniacal cobalt solution [86]. Chelating Dowex-4195 resin, in which the functional group is bis-(2-pyridylmethyl)amine has also been used in many industrial applications. For instance, it is used for nickel removal from cobalt and at several cobalt refineries [86-87].

1.3. Objectives of the study

This section outlines the background of the study, gives a short description of the ways to approach the problem and, finally, presents methods to solve the problems of this study. The limitations of the study are also discussed.

1.3.1. Background of the study

The basic goal set at the beginning of this study was to screen new potential methods for impurities removal from concentrated zinc electrolyte solutions. Zinc is produced with two different methods, hydrometallurgical and pyrometallurgical [88]. Hydrometallurgical zinc production can be divided to five steps: roasting, calcine leaching, solution purification, electrowinnig and melting [88-89]. In roasting step, zinc concentrate is fed into two parallel fluid-bed roasters, where the concentrate is roasted to calcine at a temperature of about 950 ^oC. This step is pyrometallurgy, but rest of the process is hydrometallurgy. In calcine leaching step, zinc calcine is leached with sulfuric acid to obtain concentrated $ZnSO_4$ solution in two steps: neutral and acid leaching step.

After leaching, the $ZnSO_4$ solution contains small amounts of impurities. Purification process is a three-stage process: in first step copper is removed with zinc powder (cementation), in second step rest of copper, cobalt, nickel, germanium and antimony are precipitated with As_2O_3, antimony chemicals and zinc powder, and in third step cadmium is precipitated with zinc powder [21]. The purified solution is then pumped into the electrolysis stage [88-89], where zinc is recovered from the solution using electric current [88-89]. Metallic zinc is precipitated onto aluminum cathode plates where it is allowed to build up for 36-48 hours [88-89]. Finally zinc is cast in ingots [88-89].

Because this study focuses on the solution purification step, detailed discussion is given here on the conventional methods based on usage of arsenic trioxide. Furthermore, applicability of other hydrometallurgical separation methods such as chemical precipitation, solvent extraction and ion exchange are also discussed. Typical metal ion concentrations of the concentrated $ZnSO_4$ solution before the solution purification step are shown in Table 6. Muresan [90] and Miettinen [91] have studied influence of various impurities on zinc electrowinning from sulfate electrolyte. The interferences and limiting values in zinc electrowinning are shown in Table 7.

The conventional solution purification process for concentrated zinc sulfate solutions has been studied extensively [15, 19-22, 89, 92-96]. As mentioned in Section 1.1.2, cementation is based on difference in reduction potential of metals [14] and impurity metals can be thus precipitated on the more electronegative metal surface. According to Table 8, which shows the half-cell reactions and standard reduction potentials of metals studied here, only manganese, aluminum, magnesium and calcium are more electronegative than zinc. Therefore, the other metals shown in Table 6, can be cemented with zinc dust. At Boliden Kokkola Oy zinc plant, for example, concentrated $ZnSO_4$ solutions is purified from Cu^{2+}, Ni^{2+}, Co^{2+} and Cd^{2+} ions according to Eqs 12-16 by cementation with metallic zinc dust and arsenic trioxide [89, 94]. In the beginning of the solution purification step solution temperature is about 75 ^oC [97]. Copper is precipitated first according to Eq. 12 but 50-200 mg/L copper is left in the solution to inhibit precipitation of cadmium and to accelerate precipitation of cobalt [98]. Consumption of zinc dust during precipitation of copper is usually lower than equivalent amount, because part of copper reacts to copper oxidule [21, 97-98].

$$Cu^{2+} + Zn \rightleftarrows Cu + Zn^{2+} \tag{12}$$

$$2Co^{2+} + 2As^{3+} + 5Zn \rightarrow 2CoAs + 5Zn^{2+} \tag{13}$$

$$6Cu^{2+} + 2As^{3+} + 9Zn \rightarrow 2Cu_3As + 9Zn^{2+} \tag{14}$$

$$2Ni^{2+} + 2As^{3+} + 5Zn \rightarrow 2NiAs + 5Zn^{2+} \tag{15}$$

$$Cd^{2+} + Zn \rightleftarrows Cd + Zn^{2+} \tag{16}$$

Table 6. Composition of a typical authentic $ZnSO_4$ process solution before solution purification step. Solution pH is 4.9. [99]

Ion	Concentration, mol/L
Zn^{2+}	2.5
Mg^{2+}	0.5
Mn^{2+}	0.1
Cu^{2+}	1.1·10-2
Ca^{2+}	7.8·10-3
Cl^{-}	4.0·10-3
Cd^{2+}	3.3·10-3
Al^{3+}	2.8·10-4
Co^{2+}	2.4·10-4
Ni^{2+}	2.1·10-4
Pb^{2+}	4.2·10-5
Fe^{2+}	3.2·10-5
Sb^{3+}	1.6·10-5
As^{3+}	7.5·10-6

In the second step the rest of Cu^{2+}as well as Co^{2+}, Ni^{2+}, Ge^{4+} and Sb^{3+} are precipitated according to Eqs 13-15 [21, 92, 97-98]. This step, so-called hot As_2O_3 step, involves hot As_2O_3 purification at 90 °C using zinc dust in presence of copper at pH 4 [15, 19, 22, 95-96]. An alternative method for Cu^{2+}, Co^{2+}, Ni^{2+}, Ge^{4+} and Sb^{3+} is the cold-hot purification, which also includes removal of cadmium [96]. In this method, cadmium, copper and nickel are cemented out by the addition of zinc dust at 50 °C and cobalt at 90 °C in the presence of antimony compounds, mainly Sb_2O_3 or potassium antimony tartrate (PAT) [96]. Addition of Sb_2O_3 in the second purification step has also been studied [95] because use of As_2O_3 is becoming limited due to environmental hazards, even if As_2O_3 reacts faster than Sb_2O_3 resulting less zinc consumption [20].

In the third purification step cadmium is cemented with zinc dust [21, 92, 94, 97, 98]. According to Fugleberg et al. [94], the removal of cadmium can be operated at 40 °C, whereas Yi [100] regards that the temperature generally needs to be 70 °C. After removal of cadmium, lead is removed by precipitation with $BaCO_3$ [97].

Table 7. Interferences and limiting concentrations of some impurities in zinc electrowinning. η means current efficiency [91].

Ion	Interference	Limiting concentration (mg/L)
Fe^{2+}	Lowering of η.	10-30
Cu^{2+} Cd^{2+} Pb^{2+}	Precipitation on cathode. Lowering of η.	0.1 0.3-0.6 0.5
Co^{2+} Ni^{2+}	Zinc back-dissolution. Lowering of η.	0.2 0.2
As^{3+} Sb^{3+}	Decreasing of hydrogen over-voltage. Lowering of η.	0.1 0.02
Cl^-	Corrosion of anodes.	100-300

Because of environmental and economical problems in cementation with zinc and As_2O_3, some alternative solution purification methods have also been studied [36, 101-104]. When considering the basic hydrometallurgical separation methods mentioned earlier (Section 1.1.), hydroxide precipitation can be excluded by inspection of the precipitation diagram shown in Fig. 9 [105]. According to Fig. 9 only Fe^{3+} and Cu^{2+} can be separated from concentrated $ZnSO_4$ electrolyte solutions with hydroxide precipitation but other metals shown in Table 6 cannot. On the other hand, solvent extraction and adsorption/ion exchange are potential alternatives for the conventional solution purification of concentrated $ZnSO_4$ electrolyte solutions.

Table 8. Half-cell reactions and standard reduction potentials of different metals present in zinc process solutions [106]

Half-cell reaction	E°, V
$Ca^{2+} + 2e^- \rightleftarrows Ca(s)$	-2.868
$Mg^{2+} + 2e^- \rightleftarrows Mg(s)$	-2.372
$Al^{3+} + 3e^- \rightleftarrows Al(s)$	-1.662
$Mn^{2+} + 2e^- \rightleftarrows Mn(s)$	-1.185
$Zn^{2+} + 2e^- \rightleftarrows Zn(s)$	-0.7618
$Ga^{3+} + 3e^- \rightleftarrows Ga(s)$	-0.549
$Fe^{2+} + 2e^- \rightleftarrows Fe(s)$	-0.447
$Cd^{2+} + 2e^- \rightleftarrows Cd(s)$	-0.403
$Co^{2+} + 2e^- \rightleftarrows Co(s)$	-0.28
$Ni^{2+} + 2e^- \rightleftarrows Ni(s)$	-0.257
$Pb^{2+} + 2e^- \rightleftarrows Pb(s)$	-0.1262
$Cu^{2+} + 2e^- \rightleftarrows Cu(s)$	0.3419

Solvent extraction has been studied to some extent [36, 102, 107-108] for zinc solvent purification. Friedrich et al [102] have tested LIX 84-1 (2-hydroxy-5-nonylacetophenone oxime) and a mixed aldoxime/ketoxime extractant LIX 984 (5-dodecyl-salicylaldoxime and 2-hydroxy-5-nonyl-acetophenone oxime) as a partial substitute for cementation. They have observed high selectivity of copper over zinc but for cobalt and nickel only partial extraction was achieved, and co-extraction and precipitation of zinc hydroxide was a problem [102]. According to Friedrich et al. [102], solution purification of concentrated $ZnSO_4$ electrolyte solution is made either by the hot-cold purification process or by the "reverse process. In the hot-cold process copper is extracted to the required copper concentration and cobalt and nickel are cemented with zinc dust and Sb_2O_3 at high temperature. In last step cadmium is cemented with zinc dust [102]. In the "reverse process" copper is also extracted first, then cadmium is cemented with zinc dust and cobalt and nickel are cemented in the last step with zinc dust and Sb_2O_3.

Owusu [107] has also studied copper extraction from acidic zinc sulfate leach solutions and found that LIX 622 (5-dodecyl salicylaldoxime) has high selectivity for copper over zinc. Sanberg and Hebble [36] have investigated 1,2-cyclohexanedione dioxime for selective extraction of nickel and cobalt from concentrated $ZnSO_4$ electrolyte solution. They observed in laboratory that 99 % of nickel and 93 % of cobalt could be separated when the solvent was a mixture of chloroform and isopentanol [36]. Selective separation of cadmium with solvent extraction has been studied less but Preston et al. [108] have used a mixture of tri-isobutylfosfinesulfate (TIBPS) and di-isopropylsalisylic acid (DIPSA) in xylene. They observed that cadmium could be separated selectively from zinc.

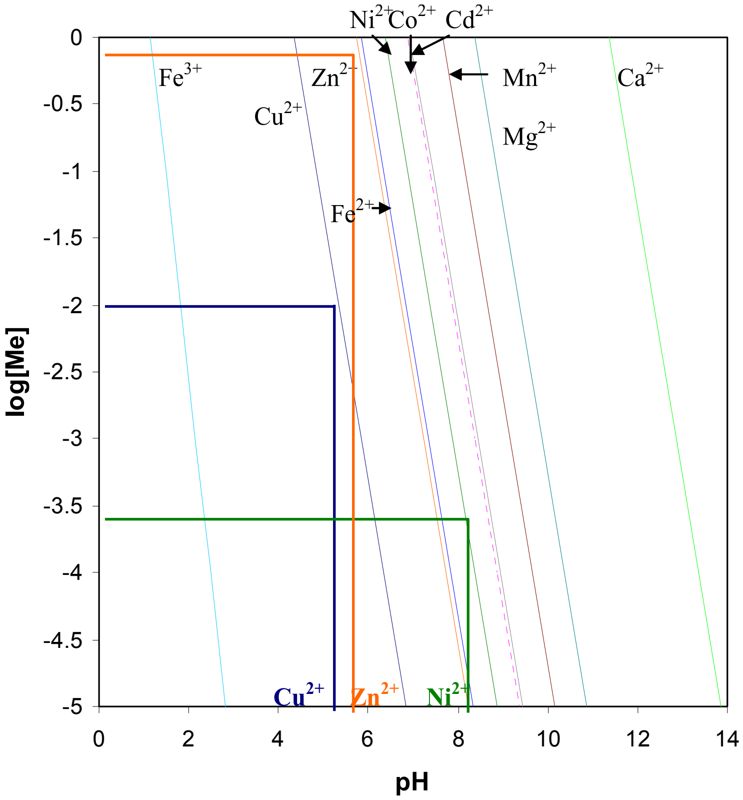

Figure 9. Precipitation diagram for metal hydroxides calculated by Eq. 3 [data from Ref. 105].

Use of solid separation materials and fixed-bed operations in solution purification of concentrated $ZnSO_4$ electrolyte solution has received only little attention. Moore [101] has patented a process for removing impurity metals such as copper, nickel, cobalt and iron from concentrated $ZnSO_4$ electrolyte solution. According to the results, copper, nickel and cobalt can be selectively separated and recovered. Nickel and cobalt can be recovered with 0.5-1 M H_2SO_4 and after that copper with 2 M H_2SO_4 [101]. The separation material was an activated carbon impregnated with salicylaldoxime [101] and it can be considered as a chelating adsorbent. Such materials are often called solvent-impregnated resins (SIR) [3]. These materials can be classified into two basic types; solvent-impregnated resins prepared by adsorption of a liquid extractant on a polymer support and resins with liquid extractant incorporated directly in the polymer matrix during polymerization (TVEX and Levextrel resins) [3]. One of the most significant disadvantages of solvent impregnated resins is low stability due to leakage of the impregnated extractant from the polymeric support. This results in a gradual loss of capacity and shortening of lifetime [109].

Simpson and Laurie [104] have used chelating ion exchangers in removal of impurities from zinc-rich waste solutions. They have reported the possibilities of Purolite S-930 resin, which contains iminodiacetic acid functionality, in a pretreatment step for zinc electrowinning after proper solution purification steps. According to their results, however, no significant gain in current efficiency was achieved but the treatment can improve the quality of the electrolyte solution, because all escaped impurities can be eliminated [104].

1.3.2. Purpose and scope of the study

The objective of this thesis is to study chelating materials as an alternative solution purification method of concentrated $ZnSO_4$ electrolyte solution. The starting point of the thesis research was the preliminary studies of Sirola [99], Pakarinen [110] and Äikäs [111], in which some highly copper-selective weakly basic chelating adsorbents were found. The main emphasis is here in the interactions between such chelating adsorbents and copper, nickel, zinc and sulfuric acid. In particular, the effect of temperature is considered important. Moreover, the binding properties and complex structures of soluble chelating ligands are studied and compared with solid-supported ligands. The problem is approached by experimental measurement and theoretical analysis of titration curves, binding isotherms, complex structures, batch uptake kinetics and dynamic column separation data. Finally, an alternative solution purification step for the concentrated $ZnSO_4$ electrolyte solution is outlined. The study is concentrated on copper and nickel removal, while the other impurities like cobalt and cadmium have been ignored.

This study is focused on two separation materials, which contain branched poly(ethyleneimine) (BPEI) and 2-(aminomethyl)pyridine (AMP), respectively. Some reference has been made to Dowex 4195 resin, which has bis-2-(pyridylmethyl)amine (bis-PMA) as the functional groups. Conventional chelating ion exchangers, such as the IDA resin, were rejected because of the unsatisfactory results obtained in the preliminary studies.

The topics discussed above are summarized in Fig. 10.

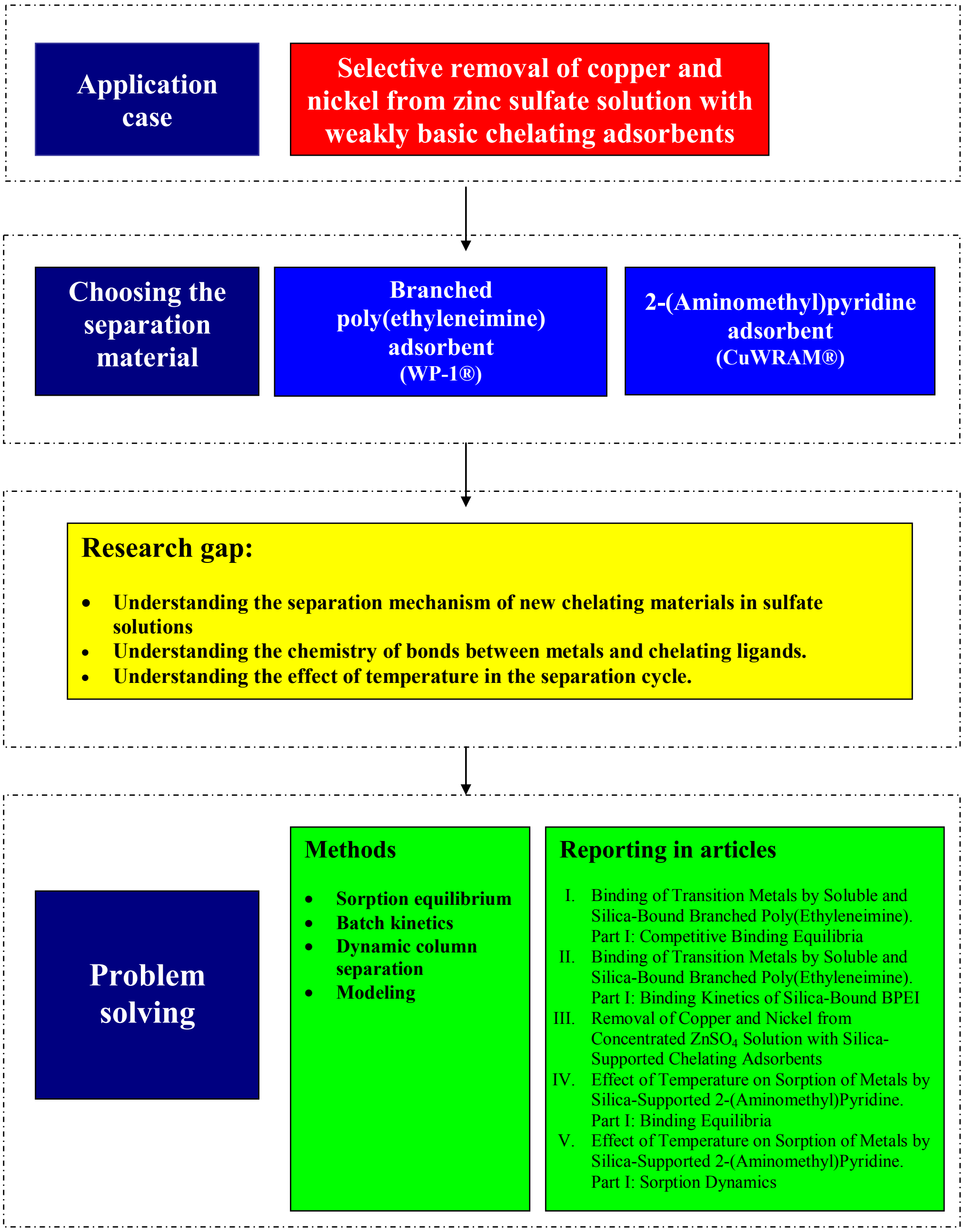

Figure 10. The contents of the thesis.

2. EXPERIMENTAL

2.1. Materials

WP-1 and CuWRAM are silica-supported chelating adsorbents in which polyamines are covalently anchored on mesoporous silica gel [112]. The polyamine, branched poly(ethyleneimine) (BPEI), itself acts as the ligand in WP-1 and it can be considered as a polymeric analogue of ethylenediamine (En) discussed earlier. The polyamine layer of CuWRAM is further functionalized to form 2-(aminomethyl)pyridine (AMP) units in the polymer chain. Structures of WP-1 and CuWRAM [113] are shown in Figure 11 and physical characteristics of the adsorbents are listed in Table 9 [III]. Two different batches of CuWRAM were used and they are designated as CuWRAM(A) (Paper [III]) and CuWRAM(B) (Paper [IV]). According to manufacturer, CuWRAM is quite new material and during the last five years the material has been further developed. This explains the marked difference in the properties of CuWRAM(A) and CuWRAM(B).

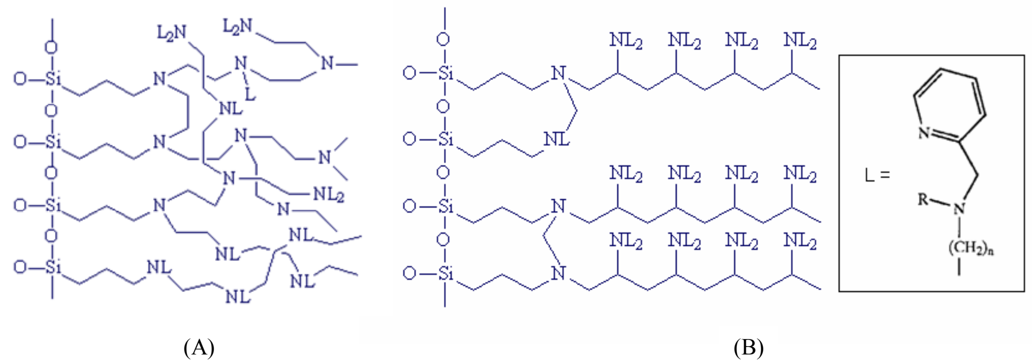

(A) (B)

Figure 11. Structures of silica-supported branched poly(ethyleneimine) (WP-1) and 2-(aminomethyl)pyridine (CuWRAM) [113].

Table 9. Properties of chelating adsorbents WP-1 and CuWRAM. The values are for unprotonated adsorbents unless indicated otherwise [I, III].

Physical property	**WP-1**	**CuWRAM(A)**	**CuWRAM(B)**
Average particle size, μm	224 ± 23	229 ± 51	n.d.
Specific surface area, m^2/g	187 ± 3	122 ± 2	145 ± 2
BJH pore volume, mL/g	0.53	0.39	0.57
Average pore size, nm	8.7	10.6	15.7
Density ρ_s, g/mL (a)	0.84	0.69^b	0.85^b
Intra-particle porosity ε_p, -	0.47	0.40	0.43
Nitrogen content, mmol/g	3.8	4.5	2.9

a: mass of dry adsorbent/volume of swollen adsorbent
b: protonated adsorbent
n.d. not determined

2.2. Methods

Because all results shown here have been obtained with similar experimental methods as explained in detail in Papers I-V, only principles and usability of the methods are discussed briefly below.

Potentiometric titrations

Potentiometric titration method is useful for determining acid-base properties of the ion exchangers and adsorbents. In this study acid-base properties of WP-1 and CuWRAM have been studied with the titration method at temperatures between 25-90 ^{o}C. By means of the titration method, acid binding capacities of the adsorbents at different acid concentrations were obtained and also relative basicities of different nitrogen atoms in the structures of the studied functional groups (BPEI and AMP) could be assessed. Furthermore, metal binding ability at different acid concentrations has been studied using different initial metal concentrations and measuring simultaneously the metal concentrations. Detailed description of the potentiometric titration experiments can be found in Papers I, III and IV [I, III-IV]

Sorption measurements

Measurement of equilibrium isotherms is used to find out effect of pH and metal concentration on metal uptake in the ion exchanger or adsorbent. In this study metal binding isotherms of WP-1 and CuWRAM have been studied at constant pH values and at 25 ^{o}C. Although this is a basic method for determining metal sorption capacities, it has one drawback; adjustment of pH is very time-consuming because of slow kinetics of the solid ion exchangers and adsorbents. Furthermore, the same results can be obtained from potentiometric titration in the presence of metals if metal concentrations of the samples are determined. Metal ion concentrations were determined by plasma emission spectroscopy (Iris Intrepid II XDL ICP-AES). The sodium interference was corrected using the same amount of Na_2SO_4 in calibration and unknown samples. The difference between duplicate analyses was less than 5 %. Detailed description of the sorption experiments can be found in Papers I, III and IV [I, III-IV]

Metal adsorption measurements by UV-VIS and reflection UV-VIS spectroscopy

If the analyzed metals are colored, UV-VIS spectrometer is useful method to analyzing of metal concentrations. In some cases metals form with organic ligands colored complexes and the method can be then used also in analyzing stoichiometry of metal-ligand complex with continuous variation method. The stoichiometry was analyzed using the spectroscopic data in the form of Job plots described in Paper [I].

In this thesis, colored copper and nickel complexes with soluble BPEI and AMP and with BPEI and AMP supported on silica (WP-1 and CuWRAM) were compared using transmission and reflection UV-VIS spectrometers at temperatures 25-90 ^{o}C, respectively. The purpose of these measurements was to find out differences in metal complexes of soluble and solid BPEI and AMP. However, detailed interpretation of the spectra was not the purpose in this study.

Binding kinetics measurements in batch system

In this study, binding kinetics of sulfuric acid, individual metals and metal pairs was measured at 25-90 ^{o}C in a batch system. The experiments were executed by allowing pH change or keeping it constant (pH-stat) and in the same time taking metals samples and analyzing them with UV-VIS or ICP spectrometers. In the case of solid adsorbents, the binding kinetics of acid and metals is so slow that this method is sufficiently accurate. However, attempts to apply the method in measuring reaction kinetics between the metals and soluble ligands were unsuccessful because of the high reaction rate.

Dynamic column separation experiments

In hydrometallurgical applications metals are removed by ion exchange or adsorption method using fixed-bed columns. In this study, laboratory-scale dynamic column experiments have been made in glass columns by measuring metal concentrations, pH and temperature from the inlet and outlet streams. Details of the experimental setup are given in Papers [III, IV]. This method is very useful and easy to execute. Furthermore, this method is not so sensitive to analytical inaccuracies as equilibrium measurements are.

Modeling

Acid and metal binding from sulfate solutions has been described using the non-ideal competitive adsorption (NICA) model reported by Kinniburgh et al. [114]. In dynamic batch and column systems, the experimental data were modeled using an approximate solution based on linear driving force (LDF) model and shrinking core model [III and V] and in some cases the results were also compared with exact numerical solution [II]. Details of the modeling are not shown in this thesis, because the author has not developed the models as was mentioned in author’s contribution in the appended publications. Models explain satisfactorily the data shown in this study and they have been helpful in explaining and illustrating the results shown in this work.

3. RESULTS AND DISCUSSION

The experimental and theoretical part of this thesis consists of materials characterization, determination of their sorption properties in model systems and testing them in a practical application. The materials used in this thesis, WP-1 and CuWRAM, are commercially available weakly basic chelating adsorbents. Their physical and chemical properties are discussed in Section 3.1. Binding of metals and complex formation abilities of these adsorbents in batch and dynamic systems are considered in Section 3.2. At the same time, comparison with analogous soluble chelating ligands is made. Effect of temperature is studied in detail only for CuWRAM, because metals precipitation discussed in Section 3.2.3. makes the use of WP-1 difficult at elevated temperatures. Suitability of these materials in removal of copper and nickel from a concentrated $ZnSO_4$ solution is discussed in Section 3.3., and in Section 2.4 the results are used to outline a future solution purification step.

3.1. Properties of the adsorbents

The physical characteristics of WP-1 and CuWRAM are quite similar but due to the chemical structures of the ligands, the acid/base properties are very different [I, III]. Titration curves of WP-1 [I] and CuWRAM(B) [IV] at temperatures of 25 °C and 60 °C are shown in Fig. 12. The new data of WP-1 at 60 °C was measured as described in Paper [III].

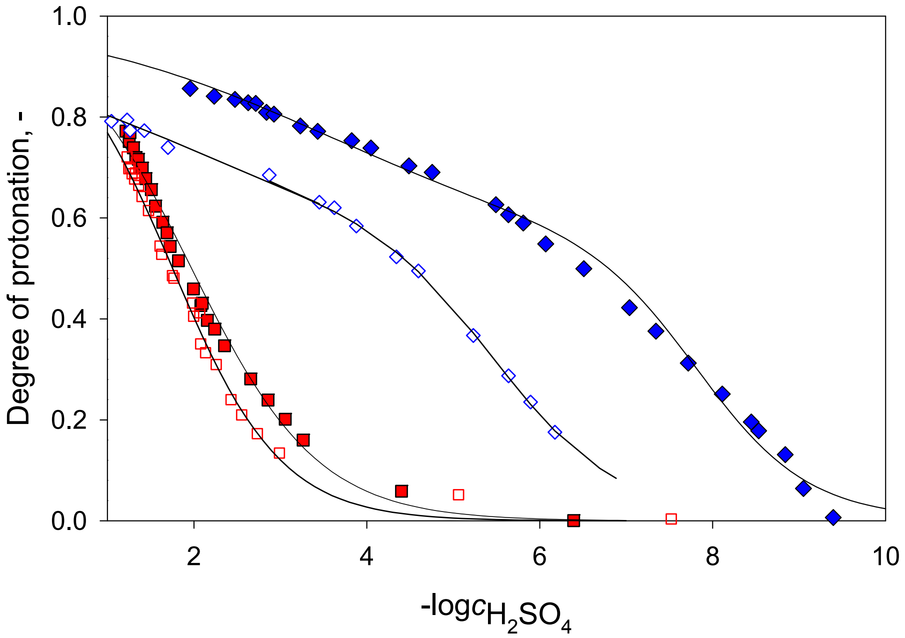

Figure 12. Titration curves of WP-1 (diamonds) [I] and CuWRAM (squares) [III]. T = 25°C (filled symbols), T = 60 °C (open symbols) and I_s = 2mol/L. The solid lines have been calculated with NICA model used in Papers [I] and [III].

According to Papers [I] and [III], WP-1 contains primary, secondary and tertiary amine groups. Acid is binding to primary and part of secondary amine groups even at very low acid concentrations, while protonation of remaining secondary and all tertiary amines is much more difficult due to steric and electrostatic hindrances. As shown in Paper I, the trend of the acid binding curve of WP-1 is qualitatively similar to that of soluble BPEI. Apparent basicity of the soluble BPEI is, however, markedly higher and the difference is considered to stem from the structure of the anchored polymer and from interactions with the silica surface.

In the case of CuWRAM, acid can bind on the nitrogen atoms in aliphatic amines of the polymer chain and in the pyridyl groups [III]. However, acid binding to aliphatic amines happens at much higher acid concentrations than expected from the behavior of unsupported AMP (see Table 5, p. 28). This is probably due to steric hindrances and the effect of neighboring charges in the polyamine chain. A distinct difference was also observed with the two batches and the apparent basicity of CuWRAM(A) was higher. Furthermore, acid binding curve of CuWRAM(B) was very similar to the acid binding curve of Dowex 4195 resin, which contains bis-PMA groups attached on polystyrene-divinylbenzene (PS-DVB) matrix. Only at low acidic conditions CuWRAM seems to be more basic. Despite of these facts, also CuWRAM(B) was assumed to contain AMP as the functional group.

Acid binding in WP-1 and CuWRAM(A) was correlated using a two-site non-ideal adsorption (NICA) model discussed in detail in Papers [I] and [III]. A simplified one-site model was used in Paper [IV] for CuWRAM(B). As can be seen from Fig. 12, the model explains reasonably well the experimental data of the both adsorbents. The estimated equilibrium parameters of WP-1 and CuWRAM are shown in Papers [I, III, IV].

According to the data in Fig. 12, increasing temperature decreases affinity for the acid indicating that acid binding in both adsorbents is exothermic and that they become more acidic with increasing temperature. The results also show that effect of increasing temperature is stronger in the case of WP-1. The binding enthalpy, ΔH_b, estimated for the more basic sites of WP-1 was -67 kJ/mol, whereas McIntyre et al. [66] have reported ΔH_b = -48 kJ/mol for En. ΔH_b was estimated using Eq. 11 and the binding constants given in Papers [I, III, IV].

In conclusion, the acid affinity of the polyamine-type adsorbent, WP-1, is much higher than that of CuWRAM having AMP as the functional ligand. Both materials appear, however, more acidic than expected from the behavior of unsupported analogues. Acid binding is an exothermic process and the apparent acidity further increases at elevated temperatures.

3.2. Binding of sulfuric acid and metal sulfates in equilibrium and dynamic systems

Metal binding in chelating adsorbents is based on the chelate-forming reaction between the metals and functional groups, and such factors as stoichiometry and structure of the metal complex, ionic strength, acid concentration and temperature are of utmost importance. Because copper and nickel form colored species in solutions and solids, UV-VIS spectroscopy is a versatile method to investigate stoichiometry and structure of their complexes with soluble and supported ligands. The Zn^{2+} ion, on the other hand, has a d^{10} electron configuration and no information can be obtained by absorbance measurements [I].

3.2.1. *Structure of copper and nickel complexes with BPEI and AMP*

Continuous variation analysis (Job plot) was used in studying stoichiometry of copper and nickel complexes with soluble BPEI (Paper [I]) and AMP (Paper [IV]). According to results [I], coordination numbers of copper and nickel with BPEI are about 4 for copper and 5-6 for nickel. These values are consistent with the conclusion that BPEI-copper complex has tetragonally distorted structure, whereas the BPEI-nickel complex has an octahedral geometry.

Stoichiometry and structure of copper and nickel complexes with AMP were studied in Paper [IV] and according to the results, copper forms 1:1 and 1:2 complexes with soluble AMP, whereas nickel can form also the 1:3 complex. However, this was observed only at pH 5, but at pH 3.5 only 1:1 and 1:2 complexes are found. This is probably due to high acid coverage in the ligand, which produces electrostatic repulsion and thus prevents formation of the 1:3 complexes.

Influence of temperature on complex formation was also studied. According to Paper [IV], temperature has only minor effect on complex formation between soluble AMP and copper and nickel in the temperature range of 25-90 ^{o}C. Similar conclusion can be drawn from Fig. 13, in which is shown the continuous variation analysis for nickel binding in soluble BPEI at pH 5 and ionic strength of 2 mol/L. These data were measured as described in Papers [I] and [IV]. Coordination number is obtained from $N_L = x_L^0/(1- x_L^0)$, where x_L^0 is the initial mole fraction of the ligand. Within the accuracy of the method, N_L appears to remain constant. Moreover, only small variation was observed in the intensity of the absorption bands suggesting that the octahedral structure remains practically unchanged.

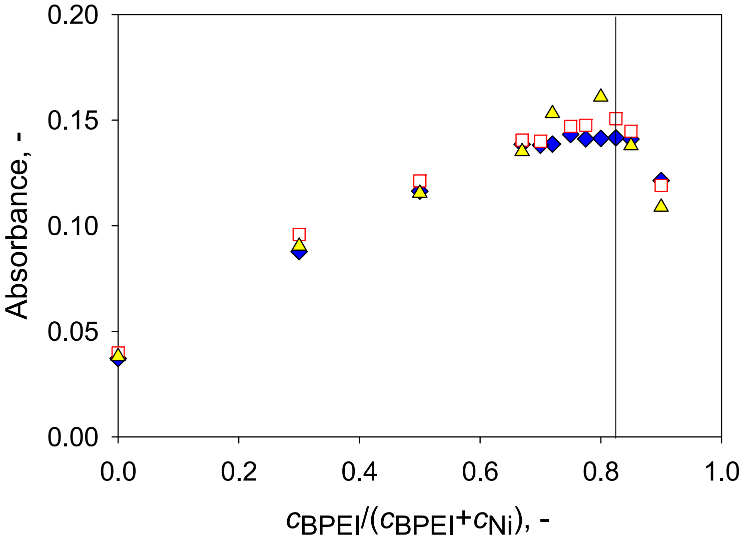

Figure 13. Continuous variation analysis for nickel binding in soluble BPEI at 25 ^{o}C (diamonds), 60 ^{o}C (squares) and 90 ^{o}C (triangles). pH 5, I_s = 2 mol/L. The vertical line illustrates the position for the 1:5 complex for soluble BPEI and nickel. The data is original for this summary.

When the absorption spectra of copper and nickel in WP-1 and CuWRAM(B) were measured, only small effect at higher temperatures was found. According to Paper [IV], temperature does not significantly affect the position of the absorption maximum in the case of copper and CuWRAM(B). Moreover, the maximum is closer to the position of the 1:1 complex of the soluble AMP ligand. The peak of nickel moves from an intermediate position between the 1:1 and 1:2 complexes towards the 1:1 complex as temperature is increasing from 25 °C to 60 °C. Temperature effect on copper complexes with WP-1 is shown in Fig. 14. The new measurements were made at pH 3 as described in Paper [IV]. The solid line represents high metal coverage at 25 °C, dashed line low coverage at 25 °C and dotted line medium coverage at 60 °C. As a result, neither coverage nor temperature seems to affect the complex formation between WP-1 and copper.

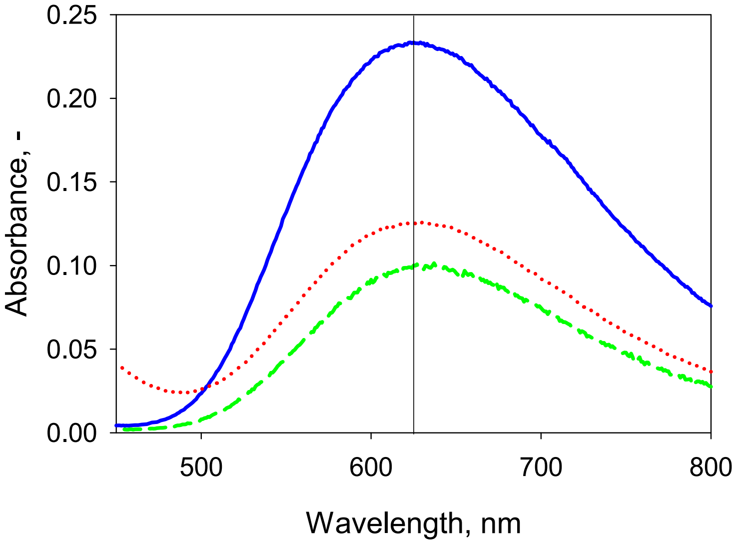

Figure 14. Temperature effect to copper complexes with WP-1. I_s = 2 mol/L. c^0 = 0.02 M $CuSO_4$, T = 25 °C and pH = 3.07 (solid line), c^0 = 0.0024 M $CuSO_4$, T = 25 °C and pH = 3.28 (dashed line) and c^0 = 0.008 M $CuSO_4$, T = 60 °C and pH = 2.96 (dotted line). The data is original for this summary. The vertical line illustrates the position of absorption maximum for the complex of soluble BPEI and copper.

The results shown above indicate that silica-supported BPEI and AMP form stable complexes with copper and nickel and many similarities are found to the behavior of soluble BPEI and AMP ligands. The stoichiometry and structure of the complexes is only slightly affected by solution conditions, coverage and temperature. The shift towards lower coordination numbers in CuWRAM at elevated temperatures seems, however, important and it is possibly related to the increasing metal uptake with increasing temperature (see Section 3.2.2.).

3.2.2. Competitive adsorption of sulfuric acid and metal sulfates in batch system

Because main emphasis of this thesis is to study metals binding in WP-1 and CuWRAM from concentrated $ZnSO_4$ process solutions, model studies with synthetic metal sulfate solutions were also made at conditions of high ionic strength. In this way the charges are effectively screened and electrostatic interactions as well as all activity coefficients can be assumed constant. Also Donnan exclusion effects in the solid materials can be neglected. Therefore, a supporting ionic strength was adjusted to 2 mol/L with Na_2SO_4. This medium is referred to as synthetic sulfate solution. The experimental data and the data correlation with the NICA model are reported in Paper [I] for WP-1 as well as in Papers [III, IV] for CuWRAM(A) and CuWRAM(B), respectively.

As mentioned in Section 3.1 and illustrated in Fig. 12, WP-1 is much more basic than CuWRAM and this difference has an important influence on metal binding properties. According to Paper [I], copper binds in WP-1 much more strongly than nickel or zinc, and the displacement of protons takes place at pH values above 2.5. For nickel and zinc the displacement region is shifted nearly two and three pH units higher. When considering the tendency of these metals to precipitate at relatively low pH values (for details, see next Section), the effective operating pH range of WP-1 is quite narrow. For this reason, the degree of protonation must be carefully controlled and this brings about problems in fixed-bed operation as will be discussed later. Because of the lower basicity, the useful pH range of CuWRAM extends in much lower values. According to the results in Paper [III], copper can displace protons from CuWRAM well below pH 1, but nickel and zinc start to bind at pH values of about 1.5 and 2.

It is assumed that copper, nickel and zinc can bind in WP-1 only via primary and part of secondary amine groups of BPEI. In CuWRAM, on the other hand, they are assumed to bind in the AMP units mainly via the pyridine nitrogen atoms. Uptake capacities of copper, nickel and zinc are for WP-1 about 0.75, 0.47 and 0.2 mmol/g at pH 5-6, respectively. The same values for CuWRAM(A) at pH 3.5 are about 1.0 mmol/g for copper and nickel, and 0.2 mmol/g for zinc. The values for CuWRAM(B) were substantially smaller, 0.6 and 0.5 mmol/g for copper and nickel, due to the substantially smaller amount of functional groups (see Table 9).

Competition between two metals in WP-1 was studied in Paper [I]. Copper selectivity coefficient was found to be about 10^4 over nickel and zinc at 25 ^{o}C, provided that solution pH is carefully adjusted to 4.5-5. Nickel binding needs a lower acid concentration and according to Paper [I], the nickel/zinc selectivity coefficient was about 10^2 at 25 ^{o}C at pH 5.5. Similar experiments were not made for CuWRAM, but the equilibrium data obtained for the process solution are discussed in Section 3.3.

Effect of temperature on copper and nickel binding in CuWRAM(B) was studied in Paper [IV]. According to the results shown in Paper [IV] and Table 10, increase of temperature from 25 ^{o}C to 90 ^{o}C markedly lowers the binding constants of copper and nickel. The enthalpy is thus negative for the chelating reactions of copper and nickel with CuWRAM, and this is in agreement with the behavior of the unsupported AMP ligand discussed in Section 1.2.3. Influence of temperature on copper and nickel adsorption capacities in CuWRAM is interesting: if temperature increases from 25 ^{o}C to 90 ^{o}C, maximum copper and nickel capacities increase from 0.6 to 0.8 mmol/g and from 0.5 to 0.8 mmol/g, respectively. The marked increase is limited to high metal loadings and elsewhere the effect was less pronounced. Increasing capacities are tentatively explained by decrease in the average coordination numbers of the metals complexes in CuWRAM. Alternatively, the increased mobility of the ligand groups at elevated temperatures may increase the number of available sites.

In conclusions, both adsorbents have high capacity for copper and increasing temperature even increases the capacities. However, because of high basicity of WP-1, it is more suitable for batch separation process, where the solution pH can be continuously adjusted to an optimum value, whereas weaker basic CuWRAM is suitable for dynamic column separation process.

3.2.3. Precipitation of basic metal sulfates

The metal precipitation problem was noticed already in a preliminary study [99]. When a concentrated metal solution was contacted with base-form WP-1 adsorbent, a precipitate was observed. The phenomenon can be explained by considering the precipitation reaction of basic metal sulfates shown in Eq. 17 [III]. Due to the high acid affinity of WP-1, the protons produced are captured by the resin and the reaction is driven to the right.

$$\mathrm{Me}^{2+}(aq) + \frac{1}{4}\mathrm{SO}_4^{2-}(aq) + \frac{3}{2}\mathrm{H_2O} \rightleftarrows \frac{1}{4}\mathrm{MeSO_4} \cdot \frac{3}{4}\mathrm{Me(OH)_2}(s) + \frac{3}{2}\mathrm{H}^+(aq) \tag{17}$$

In Fig. 15 are shown equilibrium precipitation curves of zinc and copper sulfate at temperatures of 25, 50 and 75 °C. The precipitation points of the concentrated $ZnSO_4$ process solution are also shown for the sake of comparison. According to Fig. 15, both higher concentration of metal solutions and higher temperature lower the precipitation pH. The solid lines represent calculated values and at 25 °C the estimated solubility products of copper and zinc were $\log K_{sp}(\mathrm{Cu}) = -16.1$ and $\log K_{sp}(\mathrm{Zn}) = -13.2$ (Paper [III]).

The experimental data in Fig. 15 were obtained with NaOH as the added base. Some precipitation experiments were also made with soluble BPEI at concentrations 0.05 and 0.02 mol/L. According to results shown in Fig. 15, precipitation pH of copper and nickel decreases when concentration of BPEI is increasing. Thus, BPEI makes solution more basic and basic metal sulfates precipitated more easily. Furthermore, according to Fig. 15, basic metal sulfate precipitates are also formed at lower pH values in the case of concentrated $ZnSO_4$ process solution. As was shown in Table 6, copper concentration of the concentrated $ZnSO_4$ process solutions is about 0.01 mol/L. This is assumed to decreases the basic metal sulfate precipitation points of the process solution.

In conclusion, adsorbents containing aliphatic amine groups easily cause precipitation, when contacted in base-form with concentrated metal solutions. The precipitation pH depends on concentrations of the metals and on temperature. Less basic materials like CuWRAM work at lower pH values and basic metal sulfate precipitation is not a problem, especially at ambient temperature. Some problems may occur at high temperatures and high copper concentrations even with CuWRAM.

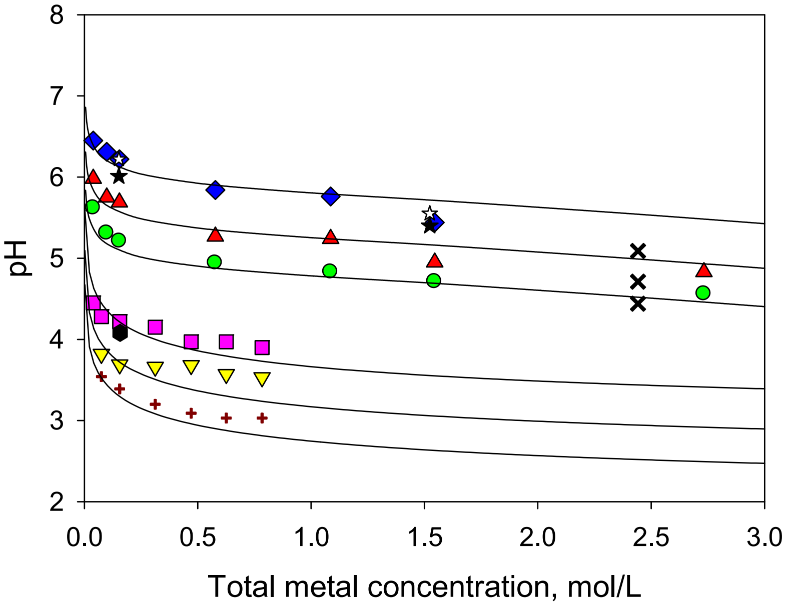

Figure 15. Equilibrium curves for precipitation of zinc basic sulfates at 25 °C (diamonds), 50 °C (triangles) and 75 °C (circles) and copper basic sulfates at 25 °C (squares), 50 °C (triangles down) and 75 °C (+). Basic sulfate precipitations of the concentrated zinc sulfate solution at 25 , 50, and 75 °C (x). 0.05 M BPEI + $ZnSO_4$ (filled stars) or $CuSO_4$ (filled hexagonal) at 25 °C and 0.02 M BPEI + $ZnSO_4$ at 25 °C (open stars) $I_s = 0$. The solid lines have been calculated as shown in Paper [III].

3.2.4. Adsorption kinetics and dynamic column separation of copper and nickel

In industrial applications the flow rates of process solutions are high and batch metal separation methods are quite impractical. As was mentioned in Section 1.1.4, ion exchange is typically executed in fixed-bed columns. The actual process can be a single-column system or a continuous multi-column system. Same process design principles apply also to chelating adsorbents. In laboratory scale, however, suitability of a given material to some separation problem is first studied using a single-column system. Even if an ion exchanger or chelating adsorbent appears useful for the purification problem according to equilibrium results, the technical potential of the material depends also on the binding rate of the separated species. Usually the rate determining step is intra-particle diffusion, external film diffusion, or in some special cases the rate of ion exchange or chemical reaction.

In this thesis the dynamics of metal binding in a WP-1 and CuWRAM were studied in Papers [II, III, V]. Adsorption rates of sulfuric acid as well as sulfates of copper, nickel and zinc were measured using batch experiments at conditions of high ionic strength. The kinetic data were correlated by means of a dynamic model, which was constructed using the following assumptions.

1. The adsorbent consists of non-swelling spherical particles of radius R and a uniform internal porosity ε_p.
2. The ligand groups are uniformly distributed in the particles.
3. Internal and external mass transfer is the rate-determining step.
4. Mass transfer inside the particles takes place by pore diffusion characterized by a diffusion coefficient D_p.
5. The diffusing species are neutral electrolytes, i.e. H_2SO_4 or $HHSO_4$ and $MeSO_4$.

Some additional data on breakthrough behavior of copper and nickel are also given. Column dynamics were modeled by combining the particle model with the overall mass balance of a dispersed-flow system as shown in Paper [III].

Batch kinetics

According to Paper [III], adsorption rate of sulfuric acid in both adsorbents can be explained rather well with a pore diffusion coefficient $D_p = 9 \cdot 10^{-10}$ m^2/s. Binding kinetics of metals is more complicated, because diffusion of the metal is coupled to diffusion of the acid via the competitive binding. As discussed in Paper [II], the rate-determining steps for WP-1 are external film diffusion or surface diffusion, when the acid concentration is low. Under certain conditions the metal uptake rate may thus be completely controlled by desorption of the acid and a bend appears in the uptake curve (see the data in Paper [II]). The observed metal adsorption rate by WP-1 is therefore controlled in a rather complicated way by desorption rate of the displaced acid. In contrast, binding kinetics of metals in CuWRAM is controlled by intra-particle diffusion, because metals are bound at significantly higher acidic concentrations. The pore diffusion coefficient estimated for the metal sulfates was $1.0 \cdot 10^{-10}$ m^2/s.

The effect of temperature on binding kinetics of copper and nickel in CuWRAM was studied in Paper [V]. Because good uptake capacity is obtained also at acidic conditions, binding rates were studied at pH 3.5. According to the results, increasing temperature gives substantially higher binding rates for all studied species. For instance, the pore diffusion coefficients of sulfuric acid and metal sulfates at 25 ^{o}C are $D_p = 9 \cdot 10^{-10}$ m^2/s and D_p, $= 1.0 \cdot 10^{-10}$ and at 90 ^{o}C they are $D_p = 17 \cdot 10^{-10}$ and $3.5 \cdot 10^{-10}$ m^2/s, respectively.

Breakthrough curves

Some column experiments with synthetic sulfate solution were made prior to the actual runs with the process solution. The purpose of these experiments was to compare the metal uptake capacities obtained in static and dynamic conditions. According to the results of Paper [V] the two values obtained for copper and CuWRAM(B) at 25 ^{o}C agree well. In the case of WP-1 the situation is more complicated. Due to metal precipitation, pH has to be adjusted below the precipitation curve shown in Fig. 15. In Fig. 16 is shown outlet profile for copper concentration and pH during loading and washing step in partially protonated WP-1 at 25 ^{o}C. Before packing in the column, WP-1 was treated with sulfuric acid so that about 50 % of the maximum capacity was protonated. According to the results shown in Fig. 16 and to the acid elution results not shown here, the copper capacity was about 0.8 mmol/g. The result agrees rather well with the equilibrium value (0.75 mmol/g at pH 5) despite the fact that the outlet pH of about 6 suggests some precipitation to be present (see the precipitation curve in Fig. 15). Consequently, even 50 % pre-protonation of WP-1 is not sufficient to completely prevent copper precipitation during the loading step. As shown in Eq. 17, precipitation reaction of the basic metal sulfate generates hydrogen ions but because of very high proton affinity of the adsorbent, solution pH cannot decrease and remains in precipitation value. Furthermore, the slight decrease in the effluent pH at copper breakthrough is due to higher copper concentration in the effluent and thus lower precipitation pH, as can be seen from Fig. 15. It is not known, whether a mixed basic salt or a mixture of Cu and Zn salts is formed. Sharp fall in the copper concentration of effluent in Fig. 16 at 82 BV is due to water rinse of the bed after loading.

In a similar way, Fig. 17 shows the outlet profiles for two loadings of 0.1 mol/L zinc in base-form WP-1 at 25 °C. Sharp fall in the zinc concentrations of effluent in Fig. 17 at bed volumes of 6 and 10 again indicates start of water rinse after loading. According to results, dynamic zinc capacity of WP-1 is about 0.8 mmol/g, which is much higher than capacity according to results obtained from equilibrium isotherms (0.2 mmol/g). The difference is probably due to precipitation of basic zinc sulfate during column loading (Section 3.2.3).

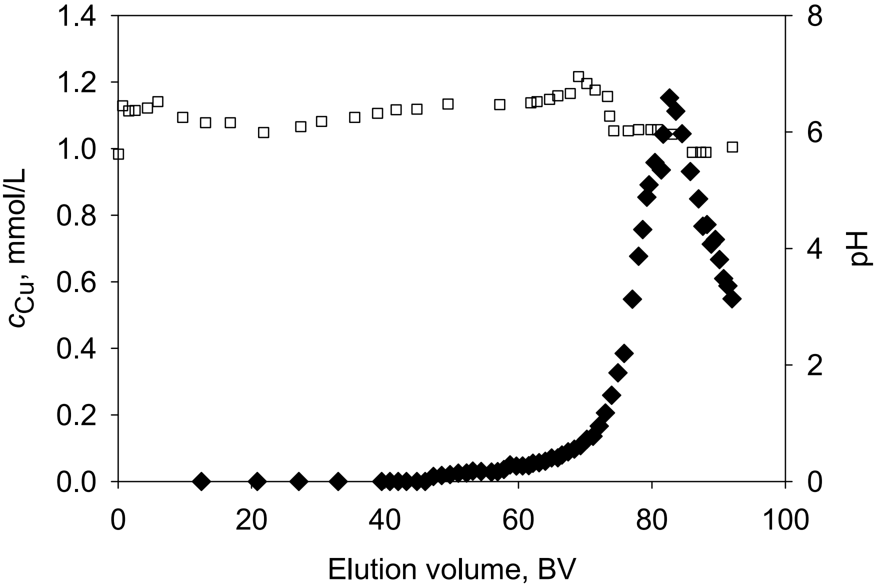

Figure 16. Outlet profiles of copper (diamonds) and pH (squares) during loading and washing steps in partially protonated WP-1. T = 25 °C, BV = 40 mL. Copper concentration in feed solution was 3.1 mmol/L, flow rate was 9 BV/h and pH 3. The data is original for this summary.

In conclusion, pore diffusion is governing the uptake rates of sulfuric acid and metal sulfates in the studied adsorbents. This set limitations for the useful range of feed flow rates in column separation of metals. According to Paper [V], increasing temperature can essentially accelerate the mass transfer rate and thus resin loading can be made at a significantly higher flow rate. When, for example, a 0.01 M $CuSO_4$ solution was loaded at 25 °C at a flow rate of 12 BV/h in a bed of CuWRAM(B), copper breakthrough took place at 20 BV. At 60 °C, on the other hand, the breakthrough point shifted to 27 BV.

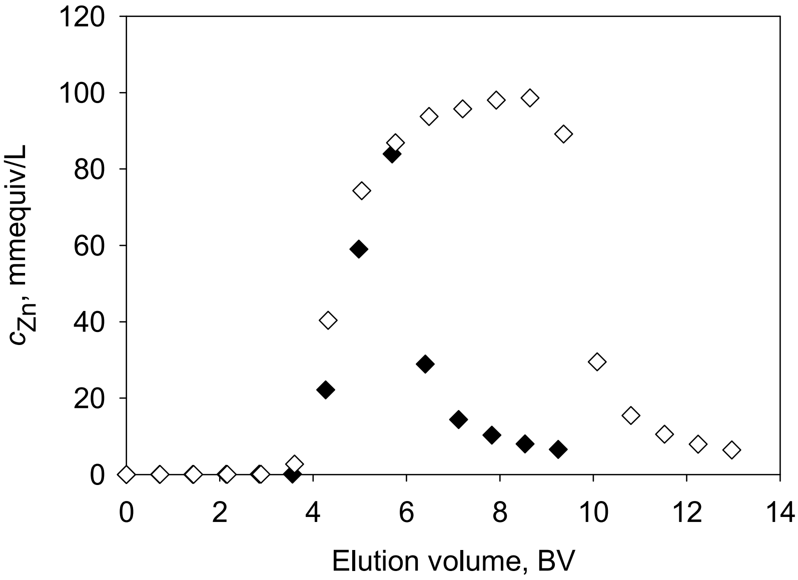

Figure 17. Outlet profiles of zinc during loading and washing step of WP-1. T = 25 °C, BV = 250 mL, zinc concentration of feed solution = 0.1 mol/L, flow rate = 4 BV/h and pH = 4.7. The open and solid symbols refer to different pulse. The data is original for this summary.

3.3. Removal of copper and nickel from concentrated $ZnSO_4$ solution

According to preliminary study of this thesis [99, 110, 111], WP-1 and CuWRAM were found to be very selective copper even in the presence of a 250-fold excess of zinc. Results obtained with the simulated sulfate solution and shown in Sections 3.1 and 3.2 indicate that copper and nickel capacities of WP-1 are high with a promising selectivity. According to Section 3.2.2, the copper and nickel capacities of CuWRAM are increasing markedly with increasing temperature. Quite surprisingly, this effect was absent in copper uptake from the process solution and the capacity was 0.5±0.05 mmol/g in the temperature range of 25-90 °C. No selectivity data were measured in the model system for CuWRAM but equilibrium experiments with the process solution (Paper IV) show that Cu/Zn, Cu/Ni and Ni/Zn selectivities at 25 °C are similar to those of WP-1.

According to Section 3.2.4, pore diffusion coefficients are reasonably high and increasing temperature further improves the mass transfer properties of both adsorbents [V]. Temperature rise from 25 °C to 90 °C was shown to result in a 3-fold increase in diffusion coefficient of metals. When considering the decreasing viscosity of the concentrated $ZnSO_4$ process solution (see Paper [V]), the actual improvement in mass transfer is even larger.

The effect of temperature on nickel removal with CuWRAM(B) from a process solution, from which copper was removed, was also studied in Paper [IV]. The results indicated that increase of temperature from 25 °C to 90 °C significantly lowers the Ni/Zn selectivity in the presence of 10000-fold zinc excess. According to Paper [IV], nickel uptake of CuWRAM at 25 °C was 0.01 mmol/g and zinc uptake was about 0.3 mmol/g. The selectivity coefficient is thus about 400. When temperature increased to 90 °C, the selectivity coefficient decreased to 200. Thus, nickel removal from the copper-free process solution with column system was studied only at 25 °C and according to results the breakthrough of nickel took place much earlier than was predicted.

Copper removal from concentrated $ZnSO_4$ process solution was studied in Papers [III] and [V]. According to the experiments made at 25 °C (Paper [III]), both adsorbents gave similar breakthrough curves but precipitation problems were observed during runs with WP-1. When loading was made in protonated WP-1, on the other hand, the copper capacity was only about 1/10 of the capacity of the base-form WP-1 [III]. No precipitation was observed with CuWRAM(A) and, moreover, no treatment was needed to render the material to base-form. The breakthrough data measured at elevated temperatures for CuWRAM(B) are shown in Paper [V] and they verify the expected trends; the uptake capacity of copper appears to increase slightly and the concentration profiles become much steeper thus allowing longer loading of the bed.

Although precipitation of the basic metal sulfates is a serious problem with WP-1, some measurements were carried out to study the effect of temperature on copper binding. In Fig. 18 are shown the outlet profiles of copper measured at 25 and 60 °C, at pH 4.9 and with a flow rate of 4 BV/h. The experimental data suggest that temperature affects copper úptake mainly via enhanced mass transfer. Therefore, the copper breakthrough shifts to much larger elution volumes and the profile becomes steeper.

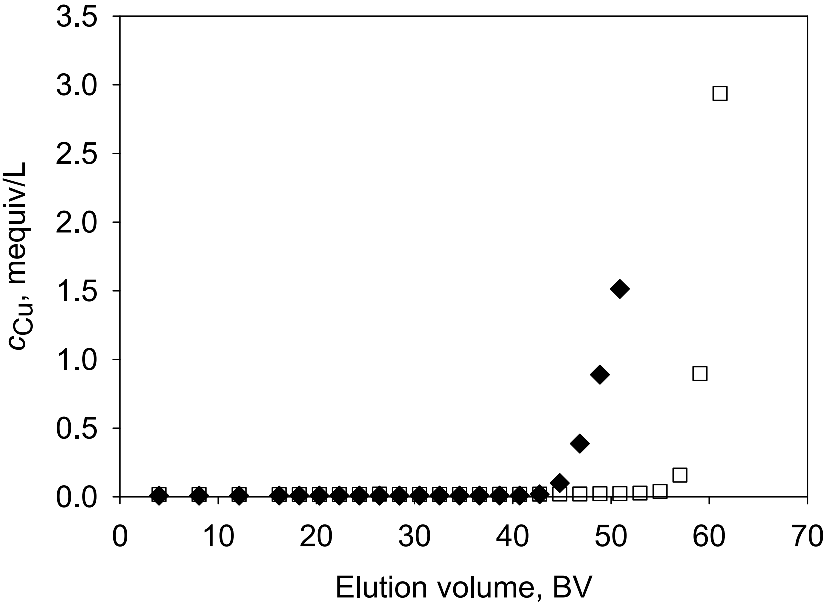

Figure 18. Outlet profiles of copper at temperatures 25 °C (diamonds) and 60 °C (squares). Feed solution was concentrated $ZnSO_4$ process solution at pH 4.9 and with a flow rate of 4 BV/h. The data is original for this summary.

In conclusion, the results mentioned in this section confirm the earlier conclusion that WP-1 is less suitable in the studied application than CuWRAM. Moreover, the favorable effect of elevated temperature on the breakthrough behavior is obvious.

3.4. Partial solution purification step for concentrated $ZnSO_4$ electrolyte solution

As discussed in Section 1.3.1, removal of impurity metals from concentrated process $ZnSO_4$ solution using ion exchangers is still at the development stage. The results of this thesis suggest, however, that copper removal is possible using the studied chelating adsorbents and that CuWRAM is much better separation material for this application than WP-1. As was shown in Paper [III], CuWRAM can be used in protonated form and still it has a high copper capacity of 0.6 mmol/g at 25 °C. The data in Paper V also shows that its performance further improves with increasing of temperature. Regeneration of the metals from CuWRAM, however, is more difficult than from WP-1 and 5 M H_2SO_4 is needed to remove metals from the adsorbent. In the case of WP-1 1 M H_2SO_4 is sufficient because of higher basicity of this adsorbent.

Separations with solid adsorbents or ion exchangers are executed in fixed-bed columns. No process design was attempted in this study but simplified flow-sheets are shown in Figs 19 and 20 for the two materials. The main purpose of these schemes is to compare the steps needed for each adsorbent. As indicated by the copper concentration in the purified solution, the proposed system is considered to substitute the first step in the conventional solution purification process (see Section 1.3.1).

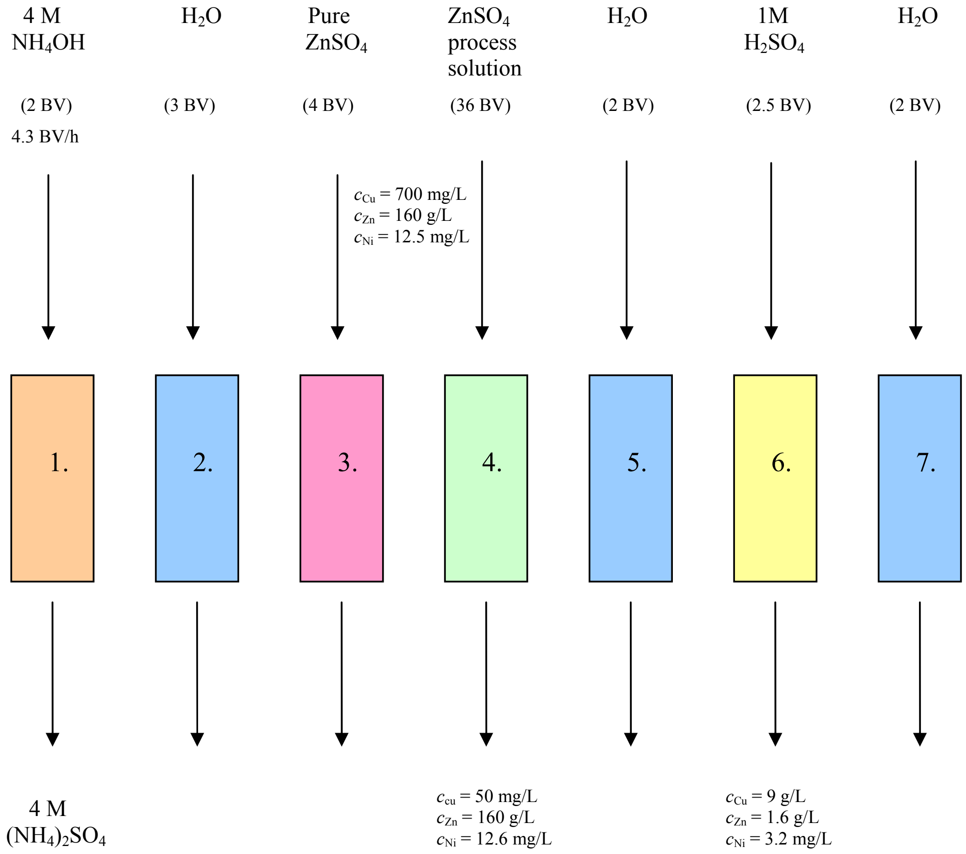

Figure 19. Process sequence for separation of copper from the process solution using WP-1 at 25 °C. The process steps are: **1.** Ammonia regeneration; **2, 5, 7.** Water rinses; **3.** Pre-treatment with pure $ZnSO_4$; **4.** Loading; **6.** Acid elution.

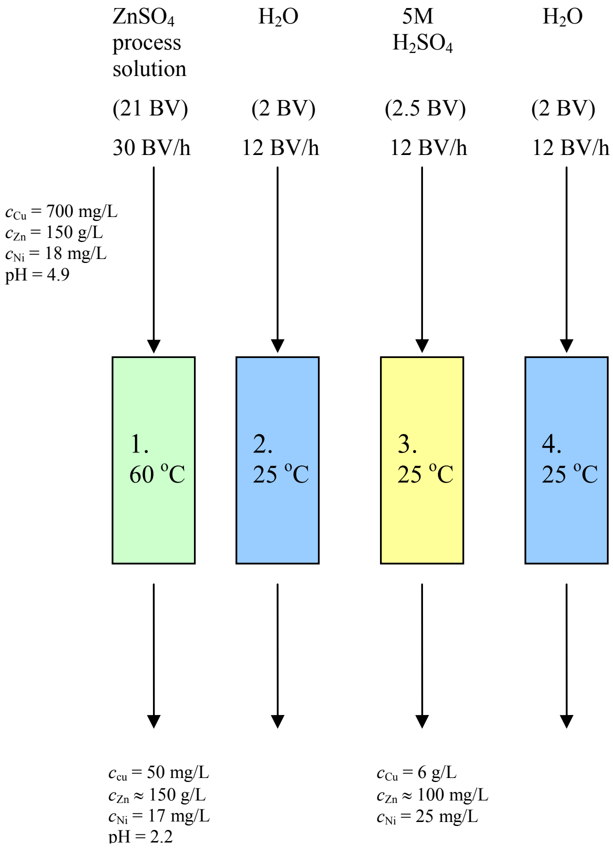

Figure 20. Process sequence for separation of copper from the process solution using CuWRAM(B). The process steps are: **1.** Loading; **2, 4.** Water rinses; **3.** Acid elution.

Comparison of Figs. 19 and 20 indicates that copper can be removed in fewer process steps when using CuWRAM. Both regeneration with NH_4OH and pre-treatment with $ZnSO_4$ solution can be omitted. The latter step was used with WP-1 to diminish the effects of precipitation. Because CuWRAM thus appears more suitable for the practical industrial application than WP-1, the following calculations were done only for CuWRAM.

When the target copper concentration in the purified solution is 50 mg/L, the flow rates in each step can be estimated from the breakthrough data. According to results shown in Paper [V], 21 BV of the process solution can be fed with flow rate of 30 BV/h and at temperature of 60 °C. In this case, about 93 % of copper contained in the original process solution is removed and subsequently recovered in the acid elution effluent. If the higher limit for the residual copper concentration, 200 mg/L, is used, the load volume increases to 35 BV. When 21 BV of the process solution has been fed, the average nickel and zinc concentrations in the effluent stream are 12 mg/L and 150 g/L, respectively.

According to results shown in Paper [III], loaded copper can be eluted from the bed with 2-2.5 BV of 5 M H_2SO_4 with a flow rate of 12 BV/h. If using the acid volume of 2.5 BV, the copper concentration in the elution stream is about 5.5 g/L, whereas nickel and zinc concentrations in the same stream are 25 and 100 mg/L, respectively. When comparing with the copper recovery of 93 %, less than 10 % of nickel is recovered in the effluent of the acid elution step. This clearly indicates that the nickel selectivity of CuWRAM in the presence of 7500-fold excess of zinc is not sufficient.

The zinc concentration, 100 mg/L, in the effluent stream of the acid elution step is only a rough estimate based on the elution data of fully saturated bed [V]. Because zinc concentration in the loading solution is as high as 150 g/L leading to rapid breakthrough of the zinc front, the dynamic zinc capacity at the cut-off point cannot be calculated from the loading step data and no verification for this value is obtained. On the basis of this value, zinc losses in the separation process can be estimated less than 0.01 %.

Washing after loading and acid elution steps was made with 2 BV of water and the wash solutions can be reused within the system but the recirculation streams are omitted from Fig. 20 for simplicity.

In practice, continuous operation is needed and the steps may take place in one or several columns or different zones, if simulated moving bed (SMB) systems are used. Actual configuration of the separation process is not considered here and Fig. 20 gives only the relative solution volumes in each step. Furthermore, comparison of various configurations and economic calculations are beyond the scope of this study.

4. SUGGESTIONS FOR FUTURE WORK

1. In this thesis copper removal from concentrated $ZnSO_4$ process solution with chelating adsorbents has been demonstrated in a single-column system and in laboratory scale. For industrial applications, the alternative solution purification step should be studied also using continuous multicolumn system, such as the SMB-process discussed in Section 1.1.4. At the same time, scale-up from laboratory to pilot scale is needed.

2. Results of this thesis clearly show that neither of the studied chelating adsorbents has sufficient selectivity for nickel, cobalt and cadmium in the presence of high concentration of zinc. However, as noticed in Section 1.2.3, the stability constants of ligands PHEN and BPY in 1:2 complexes decrease in the order Ni > Cu > Zn. Development of new solid chelating separation materials based on these or similar ligands should be considered in future studies.

5. CONCLUSIONS

In this thesis, applicability of two commercially available chelating adsorbents, WP-1 and CuWRAM, were studied in removal of copper and nickel from concentrated $ZnSO_4$ process solution. Interactions of the adsorbents with metal sulfates and sulfuric acid, effect of solid support on the binding properties and effect of temperature on the whole separation process were studied experimentally and theoretically. Incorporation of the method in the solution purification step of concentrated $ZnSO_4$ electrolyte solution was also considered, but process design was beyond the scope of this thesis.

The results of this thesis show that copper can be removed selectively from the concentrated $ZnSO_4$ process solution with both adsorbents. The selectivity for nickel and other important impurities is, however, insufficient. Use of the chelating adsorbents is thus not a realistic alternative for the entire solution purification step of concentrated $ZnSO_4$ process solution.

The marked differences observed in the behavior of the two materials mainly stem from their different acid/base properties. Because of the high acid affinity of WP-1, it has to be used in free base-form and this unavoidably leads to precipitation problems in the fixed-bed operation. On the other hand, removal of the adsorbed metals during acid elution is easy. In the case of the less basic CuWRAM the situation is different; the metals adsorb at much lower pH values and metal precipitation is not a problem. Much higher acid concentration is, however, needed to elute the bound metals but in contrast to WP-1, no treatment with a base is required before next loading step. According to the results of this study, all metals can be eluted and the other benefits of CuWRAM make it a better choice than WP-1.

Temperature was found to have a favorable effect on the fixed-bed separation. Increasing temperature results in significant improvement in intraparticle diffusion and at the same time the copper binding capacity of CuWRAM remains constant or even increases. Mass transfer is also enhanced at elevated temperatures due to decreasing viscosity of the process solution. The optimum temperature for copper removal appears to be about 60 ^{o}C.

The results obtained from comparison of silica-supported and unsupported ligands suggest that suitability of a given adsorbent for some hydrometallurgical metal separation or purification problem can be preliminarily evaluated using the soluble analogues. Only approximate results are obtained but the selectivity orders, effective pH ranges and complex structures give valuable information.

REFERENCES

1. J.E. Huheey, Inorganic Chemistry: Principles of Structure and Reactivity, 3rd Ed., Harper&Row, New York, 1983, chapters 9-11.

2. G.M. Ritcey, Solvent Extraction Principles and Applications to Process Metallurgy, G.M. Ritcey & Associates Incorporated, Canada, (2006), p. 28.

3. A. Warshawsky, J.L. Cortina and K. Jerabek, Solvent Impregnated Resin Applications on Metal Separation Process, (in Solvent Extraction and Liquid Membranes; Fundamentals and Applications in New Materials, M. Aguilar and J.L. Cortina (Eds)), Taylor & Francis, 2008, p. 303.

4. D.M. Ruthven, Principles of Adsorption and Adsorption Processes, Wiley & Sons, New York, 1984.

5. P.C. Wankat, Rate-Controlled Separations, Elsevier Applied Science, USA, 1990.

6. A. Bougen, M. Rabiller-Baudry, B. Chaufer and F. Michel, Retention of Heavy Metal Ions with Nanofiltration Inorganic Membranes by Grafting Chelating Groups, *Separ. Purif. Technol*., 25 (2001) 219-227.

7. S.K. Sikdar, J. Buckle and J. Rogut, Separation Methods for Environmental Technologies, *Environ. Progress*, 20 (2001) 1-11.

8. N. Sabba and D.E. Akretche, Use of Membranes in Copper Hydrometallurgy, *Desalination*, 193 (2006) 422-425.

9. J. Tanninen, Importance of Charge in Nanofiltration, Doctoral Thesis, Lappeenranta University of Technology, Finland, 2004.

10. G. Falk, C. Litz and R. Taylor, Wastewater Technology Fact Sheet, Chemical Precipitation, EPA Report 832-F-00-018, 2000, pp. 1-8.

11. D. Flett, Cobalt-Nickel Separation in Hydrometallurgy: a Review, *Chem. Sustainable Develop*., 12 (2004) 81-91.

12. M. Loan, G. Parkinson, M. Newman and J. Farrow, Iron Oxy-Hydroxide Crystallization in Hydrometallurgical Residue, *J. Crystal Growth*, 235 (2002) 482-488.

13. J. Monhemius, Hydrometallurgical Processing of Complex Materials, *Chem. Ind. (London),* 20 (1981) 410-420.

14. Y.J. Hsu, M.J. Kim and T. Tran, Electrochemical Study on Copper Cementation from Cyanide Liquors Using Zinc, *Electrochim. Acta*, 44 (1999) 1617-1625.

15. A. Dib and L. Makhloufi, Mass Transfer Correlation of Removal of Nickel by Cementation onto Rotating Zinc Disc in Industrial Zinc Sulfate Solutions, *Minerals Eng.*, 20 (2007) 146-151.

16. M.E. Batouti, Cementation Reactions in the Presence of Nitrogen Compounds, *J. Colloid Interface Sci.*, 263 (2003) 548-553.

17. N.E. Ghatas, Purification of Zinc Sulfate Solutions, *Canadian Patent* 1046288, 1979.

18. R.C. Kerby, Purification of Zinc Sulfate Solutions, *Canadian Patent* 1133228, 1980.

19. V. van der Pas and D.B. Dreisinger, A Fundamental Study of Cobalt Cementation by Zinc Dust in the Presence of Copper and Antimony Additives, *Hydrometallurgy*, 43 (1996) 187-205.

20. V. Singh, Technological Innovation in the Zinc Electrolyte Purification Process of a Hydrometallurgical Zinc Plant through Reduction in Zinc Dust Consumption, *Hydrometallurgy*, 40 (1996) 247-262.

21. J. Näsi, Statistical Analysis of Cobalt Removal from Zinc Electrolyte Using the Arsenic-Activated Process, *Hydrometallurgy*, 73 (2004) 123-132.

22. B.S. Boyanov, V.V. Konareva and N.K. Kolev, Purification of Zinc Sulfate Solution from Cobalt and Nickel through Activated Cementation, *Hydrometallurg*y, 73 (2004) 163-168.

23. J. Moghaddam, R. Sarraf-Mamoory, M. Ahdollahy and Y. Yamini, Purification of Zinc Ammoniacal Leaching Solution by Cementation: Determination of Optimum Process Conditions with Experimental Design by Taguchi's Method, *Separ. Purif. Technol.,* 51 (2006) 157-164.

24. G.M. Ritcey, Solvent Extraction in Hydrometallurgy: Present and Future, *Tsinghua Sci. Technol.*, 11 (2006) 137-152.

25. B. Jay, Applications for Ion Exchange Technology on Copper Hydrometallurgy, Paper presented at ALTA Copper Hydrometallurgy Conference, Australia, 1998, 1-33.

26. L.L. Tavlarides, J.H. Bae and C.K. Lee, Solvent Extraction, Membranes, and Ion Exchange in Hydrometallurgical Dilute Metal Solutions, *Separ. Sci. Technol.*, 22 (1987) 581-617.

27. F. Helfferich, Ion Exchange, Dover Publications Inc., USA, 1995, p. 154, 253.

28. H. Leinonen, Removal of Harmful Metals from Metal Plating Waste Waters using Selective Ion Exchangers, Doctoral Thesis, University of Helsinki, 1999.

29. O. Hamdaoui, Removal of Copper(II) from Aqueous Phase by Purolite C100-MB Cation Exchange Resin in Fixed Bed Columns: Modelling, *J. Hazard. Mater.*, 161 (2009) 737–746.

30. B. Jay, Applications of Ion Exchange Resins in Hydrometallurgy, Paper presented at ALTA Solvent Extraction/Ion Exchange World Summit Conference, Australia, 2003, 1-11.

31. Ion Exchangers, K. Dorfner (Ed), De Gruyter, Berlin, 1991, p. 1061-1072.

32. M. Streat and D. Naden, Ion Exchange and Sorption Processes in Hydrometallurgy, Critical Reports on Applied Chemistry, John Wiley & Sons, 1987.

33. B.A. Bolto and L. Pawlowski, Wastewater Treatment by Ion-Exchange, E. & F.N. Spon Ltd, London, 1987.

34. J.W. Patterson, Industrial Wastewater Treatment Technology, Butterworth Publishers, USA, 1985.

35. A. Dabrowski, Z. Hubicki, P. Podkoscielny and E. Robens, Selective Removal of the Heavy Metal Ions from Waters and Industrial Wastewaters by Ion-Exchange Method, *Chemosphere*, 56 (2004) 91-106.

36. G.S. Sandberg and T.L. Hebble, Cobalt and Nickel Removal from Zinc Sulfate Electrolyte by Solvent Extraction and Precipitation Techniques, United States Department of the Interior, 1978.

37. J.A. Davies, C.M. Hockensmith, V.Y. Kukushkina and Y.N. Kukushkin, Synthetic Coordination Chemistry; Principles and Practice, World Scientific, Singapore-New Jersey, 1996.

38. Chemical of the Week, Chelates and Chelating Agents, http://scifun.chem.wisc.edu/CHEMWEEK/Chelates/Chelates.html, referred to 8.8.2009.

39. V. Vallet, U. Wahlgren and I. Grenthe, Chelate Effect and Thermodynamics of Metal Complex Formation in Solution: A Quantum Chemical Study, *J. Am. Chem. Soc.*, 125 (2003) 14941-14950.

40. M. Calvin and R.H. Bailes, Stability of Chelate Compounds II. Polarographic Reduction of Copper Chelates, *J. Am. Chem. Soc.*, 68 (1946) 949-954.

41. G. Schwarzenbach, Metallkomplexe mit Polyaminen IX. Die Interpretation der Stabilitätskonstanten der Silberkomplexe, *Helv. Chim. Acta,* 291 (1952) 2344 (in German).

42. F.A. Cotton and G. Wilkinson, Advanced Inorganic Chemistry, 5th Ed., John Wiley & Sons, USA, 1988.

43. A. von Zelewsky, Stereochemistry of Coordination Compounds, John Wiley & Sons, USA, 1996.

44. Complex (Chemistry), http://en.wikipedia.org/wiki/Complex_(chemistry), referred to 8.8.2009.

45. M.J. Hudson, Coordination Chemistry of Selective Ion Exchange Resins (in: Ion Exchange: Science and Technology, A.E. Rodrigues (Ed.)), Publisher Martinus Nijhoff, 1986, Dordrecht, 35-66

46. W.W. Porterfielf, Inorganic Chemistry; a Unified Approach, Addison-Wesley Publishing Company, Inc., USA, 1984.

47. R.G. Pearson, Hard and Soft Acids and Bases, *J. Am. Chem. Soc.*, 85 (1963) 3533-3539.

48. R.G. Pearson, Hard and Soft Acids and Bases HSAB, Part I: Fundamental Principles, *J. Chem. Ed.*, 45 (1968) 581-586.

49. R.G. Pearson, Hard and Soft Acids and Bases HSAB, Part II: Underlying Theories, *J. Chem. Ed.*, 45 (1968) 643-648.

50. M Eigen and K. Tamm, Schallabsorption in Elektrolytlösungen als Folge chemischer Relaxation. II. *Z. Elektrochem.*, 66 (1962), 107 (in German).

51. H. Diebler, Kinetics of Elementary Steps in Metal Complex Formation Reactions, Proc. 3rd Symp. Coord. Chem., M. Beck (Ed.), Debrecen, 1970, 53-76.

52. R.G. Parr and R.G. Pearson, Absolute Hardness: Companion Parameter to Absolute Electronegativity, *J. Am. Chem. Soc.*, 105 (1983) 7512-7516.

53. H.M.N.H. Irving and R.J.P Williams, The Stability of Transition-Metal Complexes, *J. Chem. Soc*., (1953) 3192-3210.

54. J.P. Williams, The Stability of the Complexes of the Group IIA Metal Ions, *J. Chem. Soc*, (1952) 3770-3778.

55. A.E. Martell and R.D. Hancock, Metal Complexes in Aqueous Solutions, Plenum Press, New York, 1996, chapter 3.

56. E. Garcia-Espana, F. Nuzzi, A. Sabatini, A. Vacca, Reactions of 2-(Aminomethyl)Pyridine with Hydrogen Ion and Divalent Transition Metal Ions. I. Equilibrium Constants, *Gazz. Chim. Ital.*, 115 (1985) 607-611.

57. C.V. Banks and R.I. Bystroff, Stability Orders in Transition Metal-1,10-Phenanthroline Complexes, *J. Am. Chem. Soc.*, 81 (1959) 6153-6158.

58. N. McCann, G.A. Lawrence, Y-M. Neuhold and M. Maeder, Complexation Kinetics of Copper(II) and Nickel(II) with Macrocycles: Identification of an Outer-Sphere Chelate Effect, *Inorg. Chem*., 46 (2007) 4002-4009.

59. D.B. Rorabacher, The Kinetics of Formation and Dissociation of the Monoamine Complexes of the Divalent, First-Row Transition Metal Ions, *Inorg. Chem.*, 5 (1966) 1891-1899.

60. I. Fabian and H. Diebler, Kinetics of the Consecutive Binding of Bipyridyl Ligands and of Phenanthroline Ligands to Copper(II), *Inorg. Chem.*, 26 (1987) 925-928.

61. R.W. Taylor, H.K. Stepien and D.B. Rorabacher, Kinetics of Aquanickel(II) Ion Reaction with Ethylenediamine. Evidence of the Internal Conjugate Base Effect and Intramolecular Hydrogen Bonding, *Inorg. Chem.*y, 13 (1974) 1282-1289.

62. M. Grant, H.W. Dodgen and J.P. Hunt, Kinetics of Water Exchange between Solvent and Aquobipyridylnickel(II) Complexes, *J. Am. Chem. Soc.*, 92 (1970) 2321-2323.

63. A.E. Martell and R.J. Motekaitis, Determination and Use of Stability Constants, VCH Publishers, 1988, p 146.

64. A.K. Sengupta and Y. Zhu, Metals Sorption by Chelating Polymers: a Unique Role of Ionic Strength, *AIChE J.*, 38 (1992) 153-157.

65. A. Agrawal, K.K. Sahu and J.P. Rawat, Kinetic Studies on the Exchange of Bivalent Metal Ions on Amberlite IRC 718 – an Iminodiacetate Resin, *Solvent Extract. Ion Exch.*, 21 (2003) 763-782.

66. G.H. McIntyre , B.P. Block and W.C. Fernelius, A Thermodynamic Study of Some Metal-Amine Coordination Compounds, *J. Am. Chem. Soc.*, 81 (1959) 529-535.

67. D.E. Goldberg and W.C. Fernelius, The Thermodynamic Study of Some Coordination Complexes of Metal Ions with Diprotic Nitrogen Compounds Containing One Heterocyclic Nitrogen Atom, *J. Phys. Chem.*, 63 (1959) 1246-1249.

68. R.L. Davies and K.W. Dunning, The Heats of Formation of Complex Ions Containing Bipyridyl, *J. Chem. Soc.*, (1965) 4168-4185.

69. G. Anderegg, Pyridinderivative als Komplexbildner VI. Reaktionsentalpie und –Entropie bei der Bildung der Metallkomplexe von 1,10 Phenanthrolin und α,α-Dipyridyl, *Helv. Chim. Acta*, 46 (1963) 2813-2822 (in German).

70 M. Pesavento, R. Biesuz, M. Gallorini and A. Profumo, Sorption Mechanism of Trace Amounts of Divalent Metal Ions on a Chelating Resin Containing Iminodiacetate Groups, *Anal. Chem.*, 65 (1993) 2522-2527.

71. D. Atzei, T. Ferri, C. Sadun, P. Sangiorgio and R. Caminiti, Structural Characterization of Complexes Between Iminodiacetic Blocked on Styrene-Divinylbenzene Matrix (Chelex 100 Resin) and Fe(III), Cr(III) and Zn(II) in Solid Phase by Energy Dispersive X-ray Diffraction, *J. Am. Chem. Soc.,* 123 (2001) 2552-2558.

72. A. Agrawal and K.K. Sahu, Influence of Temperature on the Exchange of Alkaline Earth and Transition Metals on Iminodiacetate Resin, *Solvent Extract. Ion Exch.*, 23 (2005) 265-287.

73. R.T. Herrin, A.W. Andren and D.E. Armstrong, Determination of Silver Speciation in Natural Waters. 1. Laboratory Tests of Chelex-100 Chelating Resin as a Competing Ligand, *Environ. Sci. Technol.* 35 (2001) 1953-1958.

74. Z. Zainol, The development of a Resin-in-Pulp Process for the Recovery of Nickel and Cobalt from Laterite Leach Slurries, Doctoral Thesis, Murdoch University, Australia, 2005.

75. A.W. Trochimczuk and M. Streat, Novel Chelating Resins with Aminothiophosphonate Ligands, *React. Funct. Polymers*, 40 (1999) 205-213.

76. J. Lehto, K. Vaaramaa and H. Leinonen, Ion Exchange of Zinc on an Aminophosphonate-Chelating Resin, *React. Funct. Polymers*, 33 (1997) 13-18.

77. R. Kiefer and W.H. Höll, Sorption of Heavy Metals onto Selective Ion-Exchange Resins with Aminophosphonate Functional Groups, *Ind. Eng. Chem. Res*. 40 (2001) 4570-4576.

78. Y. Zhu, Chelating Polymers with Nitrogen Donor Atoms: Their Unique Properties in Relation to Heavy Metals Sorption and Ligand Exchange, Doctoral Thesis, Leigh University, USA, 1992.

79. D. Zhang, Polymer Ligand Exchange: A New Approach toward Enhanced Separation of Environmental Contaminants, Doctoral Thesis, Leigh University, USA, 1997.

80. R.R. Grinstead, Copper-Selective Ion-Exchange Resin with Improved Iron Rejection, *J. Metals*, (1979) 13-16.

81. R.R. Grinstead, New Developments in the Chemistry of XFS 4195 and XFS 43084 Chelating Ion Exchange Resins, *Ion Exch. Technol*., (1984) 509-518.

82. R.R. Grinstead, Selective Adsorption of Copper, Nickel, Cobalt and Other Transition Metal Ions from Sulphuric Acid Solutions with the Chelating Ion Exchange Resin XFS 4195, *Hydrometallurgy*, 12 (1984) 387-400.

83. C.V. Diniz, F.M. Doyle and V.S.T. Ciminelli, Effect of pH on the Adsorption of Selected Heavy Metal Ions from Concentrated Chloride Solutions by the Chelating Resin Dowex M-4195, *Separ. Sci. Technol*., 37 (2002) 3169-3185.

84. K.C. Jones and R.R. Grinstead, Properties and Hydrometallurgical Applications of Two Chelating Ion Exchange Resins, *Chem. Ind.*, (1977) 637-641.

85. F.D. Mendes and A.H. Martins, Selective Sorption of Nickel and Cobalt from Sulphate Solutions Using Chelating Resins, *Int. J. Mineral Proces.*, 74 (2004) 359-371.

86. M.H. Kotze and J.P. Wyethe, Existing and Potential Ion Exchange Applications in the Nickel, Cobalt and Copper Industries, Paper presented at ALTA Solvent Extraction/Ion Exchange World Summit Conference, Australia, 2003, 1-17.

87. M.H. Kotze, J.P. Wyethe and B.R. Green, Review of Ion Exchange Processes for the Base Metal Industry, Paper presented at ALTA Ni/Co Conference, Australia, 2001, 1-26.

88. Kirk-Othmer Encyclopedia of Chemical Technology, Vol. 24, 3th Ed., John Wiley & Sons, Inc., New York, 1985.

89. H. Takala, Leaching of zinc concentrates at Outokumpu Kokkola plant, *Erzmetals,* 52 (1999) 37-42.

90. L. Muresan, G. Maurin, L. Oniciu and D. Gaga, Influence of Metallic Impurities on Zinc Electrowinning from Sulfate Electrolyte, *Hydrometallurgy*, 43 (1996) 345-354.

91. V. Miettinen, Impurities in the Solvent Extraction of Zinc, Master's Thesis, Lappeenranta University of Technology, 2004, p. 6 (in Finnish).

92. S. Fugleberg, Finnish Expert Report on Best Available Techniques in Zinc Production, *The Finnish Environ.* 315, 1999 1-45.

93. S. Fugleberg, R. Rantanen, V. Sipilä and A. Järvinen, High Conductivity Copper and Aluminum Alloys, Proc. TMS-AIME Annual Meeting, 113th, Los Angeles, (1984) 1-8.

94. S. Fugleberg, A. Järvinen, A. Yllö, Recent Development in Solution Purification at Outokumpu Zinc Plant, Kokkola, ZINC '93, Hobart, Australia, (1993) 1 – 20.

95. R. Xu, K. Ma and Z. Guo, Activation Mechanism of Sb_2O_3 during Removal of Cobalt from Zinc Sulphate Solution, *Hydrometallurgy*, 82 (2006) 150-153.

96. R. Raghavan, P.K. Mohanan and S.K. Verma, Modified Zinc Sulphate Solution Purification Technique to Obtain Low Levels of Cobalt for the Zinc Electrowinning Process, *Hydrometallurgy*, 51 (1999) 187-206.

97. H. Takala, Sinkin hydrometallurginen valmistus, Laboratoriotekniikoiden koulutus, PTOL, Pori, 1993 1-13 (in Finnish).

98. J. Näsi and A. Sorsa, Jatkuvatoimisen liuospudistuksen pilot-prosessin mallinnus ja prosessikehitys, Report B 36, Oulu University, 2002 1-13 (in Finnish).

99. K. Sirola, Separation of Impurities from Zinc Sulphate Solutions Using Selective Ion Exchangers, Master's Thesis, Lappeenranta University of Technology, 2003, 1-106 (in Finnish).

100. L. Yi, Experimental Study on Purification of $ZnSO_4$ Solution in Zhuzhou Smelter, Hydrometallurgy Conference, China, 1998.

101. R.H. Moore, Sorbate Extraction of Metallic Values from Aqueous Leach Solutions, *U.S. Patent,* No. 3682589, 1972.

102. B. Friedrich, J. Krüger and G.M. Bernal, Alternative Solution Purification in the Hydrometallurgical Zinc Production, European Metallurgical Conference, Germany, 2001 179-197.

103. R.V. Pammenter, M.G. Kershaw and R.C.A. Maughan, The Elimination of Nickel from Zinc Plant Solutions using Dimethylglyoxime, The Aus.I.M.M. Conference, 1977 291-298.

104. C. Simpson and S.H. Laurie, Ion Exchange Studies on Zinc-Rich Waste Liquors, *Hydrometallurgy,* 51 (1999) 335-344.

105. A. Ringbom, Complexation in Analytical Chemistry, Wiley & Sons, New York, 1963 p. 339-347.

106. P. Vanysek, Electrochemical series, (in: CRC Handbook of Chemistry and Physics, 83rd ed.), CRC Press, Boca Raton, 2003.

107. G. Owusu, Selective Extraction of Copper from Acidic Zinc Sulfate Leach Solution Using LIX 622, *Hydrometallurgy*, 51 (1999) 1-8.

108. J.S. Preston, J.H. Patrick and G. Steinbach, The Selective Solvent Extraction of Cadmium by Mixtures of Carboxylic Acids and Trialkylphosphine Sulphides. Part 2. Practical Applications in the Separation of Cadmium from Zinc and Nickel, *Hydrometallurgy*, 36 (1994) 141–158.

109. D. Muraviev, L. Ghantous and M. Valiente, Stabilization of Solvent Impregnated Resin Capacities by Different Techniques, *React. Funct. Polymers*, 38 (1998) 259-268.

110. J. Pakarinen, Removal of Nickel and Cobalt from Zinc Sulfate Solution by Ion Exchange, Master's Thesis, Lappeenranta University of Technology, 2004, 1-86 (in Finnish).

111. L.-M. Äikäs, Properties and Hydrometallurgical Applications of Pyridyl Group Containing Separation Materials, Master's Thesis, Lappeenranta University of Technology, 2005, 1-111 (in Finnish).

112. E. Rosenberg, R.J. Fischer, Materials and Methods for the Separation of Copper Ions and Ferric Iron in Liquid Solutions, *U.S. Patent* no. 2004/0000523 A1 (2004).

113. S.T. Beatty, R.J. Fischer, D.L. Hagers, E.A. Rosenberg, A Comparative Study of the Removal of Heavy Metal Ions from Water Using a Silica-Polyamine Composite and a Polystyrene Chelator Resin, *Ind. Eng. Chem. Res*., 38 (1999) 4402–4408.

114. D.G. Kinniburgh, H. van Riemsdijk, L.K. Koopal, M. Borkovec, M.F. Benedetti, M.J. Avena, Ion Binding to Natural Organic Matter: Competition, Heterogeneity, Stoichiometry and Thermodynamic Consistency, *Colloids Surf. A* 151 (1999) 147–166.

APPENDICES

Scientific publications I-V

Scientitic publications I-V

I

Reprinted from Colloids and Surfaces A: Physicochemical Engineering Aspects, Vol. 296, Laatikainen, M., Sirola K., Paatero E., *Binding of transition metals by soluble and silica-bound branched poly(ethyleneimine). Part I: Competitive binding equilibria*, 191-205, Copyright (2007), with permission from Elsevier.

http://dx.doi.org/10.1016/j.colsurfa.2006.09.044

II

Reprinted from Journal Colloids and Surfaces A: Physicochemical Engineering Aspects, Vol. 296, Sirola K., Laatikainen, M., Paatero E., *Binding of transition metals by soluble and silica-bound branched poly(ethyleneimine). Part II: Binding kinetics in silicabound BPEI*, 158-166, Copyright (2007), with permission from Elsevier.

http://dx.doi.org/10.1016/j.colsurfa.2006.09.040

III

Reprinted from Separation and Purification Technology, Vol. 64, Sirola K., Laatikainen, M., Lahtinen, M., Paatero E., *Removal of copper and nickel from concentrated ZnSO4-solutions with silica-supported chelating adsorbents*, 88-100, Copyright (2008), with permission from Elsevier.

http://dx.doi.org/10.1016/j.seppur.2008.08.001

IV

Reprinted from Reactive and Functional Polymers, Sirola K., Laatikainen, M., Paatero E., *Binding of copper and nickel in silica-supported 2-(aminomethyl)pyridine at elevated temperatures. Part I: Binding equilibri***a (In Press),** Copyright (2009), with permission from Elsevier.

> (Effect of temperature on sorption of metals by silica-supported 2-(aminomethyl)pyridine. Part I: Binding equilibria *Reactive and Functional Polymers, Volume 70, Issue 1, January 2010, Pages 48-55* Katri Sirola, Markku Laatikainen, Erkki Paatero

http://dx.doi.org/10.1016/j.reactfunctpolym.2009.10.003

V

Reprinted from Reactive and Functional Polymers, Sirola K., Laatikainen, M., Paatero E., *Binding of copper and nickel in silica-supported 2-(aminomethyl)pyridine at elevated temperatures. Part II: Binding dynamics* **(In Press**), Copyright (2009), with permission from Elsevier.

> (Effect of temperature on sorption of metals by silica-supported 2-(aminomethyl)pyridine. Part II: Sorption dynamics *Reactive and Functional Polymers*, *Volume 70, Issue 1*, *January 2010*, *Pages 56-62* Katri Sirola, Markku Laatikainen, Erkki Paatero)

http://dx.doi.org/10.1016/j.reactfunctpolym.2009.10.005

Elsevier

http://www.elsevier.com/wps/find/journal_browse.cws_home?q=1&SH1Code=&pseudotype=&sortBy=Title&letter=C